Energy for Sustainable Development 79 (2024) 101409

Contents lists available at ScienceDirect

Energy for Sustainable Development

journal homepage: www.journals.elsevier.com/energy-for-sustainable-development

Experimental characterization of a foldable solar cooker with a trapezoidal cooking chamber and adjustable reflectors

Tariku Negash Demissie [a], Sebastiano Tomassetti [a,*], Claudia Paciarotti [a], Matteo Muccioli [b], Giovanni Di Nicola [a,c], Celestino Rodrigues Ruivo [d,e]

[a] Marche Polytechnic University, Department of Industrial Engineering and Mathematical Sciences, Via Brecce Bianche 12, 60131 Ancona, Italy
[b] Studio MUMA, Via Eugenio Curiel 66 R, 47922, Rimini, Italy
[c] Construction Technologies Institute, National Research Council (ITC-CNR), Corso Stati Uniti 4, 35127 Padova, Italy
[d] Department of Mechanical Engineering, Institute of Engineering, University of Algarve, Campus da Penha, 8005-139 Faro, Portugal
[e] ADAI, Department of Mechanical Engineering, Rua Luís Reis Santos, Pólo II, 3030-788 Coimbra, Portugal

ARTICLE INFO

Keywords:
Solar cooker
Foldable
Adjustable reflectors
Experimental test
Humanitarian camps

ABSTRACT

In this study, a portable and easy-to-construct solar cooker is presented as an alternative to traditional cooking methods to be used in humanitarian contexts in order to face the issue of humanitarian goods transport and storage. The prototype consists of a trapezoidal cooking chamber and adjustable reflector panels made of inexpensive and readily available materials. The solar cooker was designed to be foldable and transportable by using lightweight materials. In fact, the folded prototype is compact, having a mass of 7 kg. The thermal performance and optical performance of the proposed cooking appliance were evaluated through several experiments conducted without load and with load. The tests were done by using a black pot enclosed with a glass bowl or a plastic bag. During the tests without load, the highest recorded temperature was 149.38 °C. The time needed to bring 1 kg of water from 40 °C until 90 °C was on average 114 min for the glass enclosure tests and 132 min for the plastic enclosure tests. The prototype loaded with 1 kg of glycerin took the same average time of 121 min to reach 105 °C from 40 °C for both glass and plastic enclosure tests. The average values of cooking power, derived using Hottel-Whillier-Bliss formulation with a reference global normal solar irradiance for the clear sky condition, are estimated as 26.0 W for the water tests using the glass enclosure and 31.8 W for the glycerin tests with the glass enclosure. Finally, the cooking performance of the prototype was evaluated by cooking common foods (i.e., tomatoes, rice, potatoes). The average cooking times for tomatoes, rice, and potatoes were always lower than two hours, a value consistent with the cooking times of different box solar cookers.

Introduction

According to estimates provided by the United Nations, there are 339 million people all over the globe who need humanitarian help, and 103 million people are displaced from their homes (UN Ocha, 2022). The vast majority of these displacements that take place across the globe occur as a direct result of natural disasters, severe weather events like floods and drought, conflicts, and wars. One of the basic needs of these people is access to instruments for clean cooking. Indeed, the smoke caused by inefficient stoves and fuels may lead to a number of health problems, including illnesses of the respiratory system.

In Sub-Saharan Africa, as much as 85 % of the people in refugee camps still rely on inefficient and unsustainable traditional cooking stoves that produced 14.3 million tons of CO_2 emissions in 2014 (Rivoal & Haselip, 2017). Each year, more than 3.9 million people pass away due to respiratory issues related to household indoor air pollution caused by solid fuel use, with an estimated 20,000 displaced individuals dying prematurely (Lahn & Grafham, 2015; Smith et al., 2014).

In certain parts of the world, women have to travel for hours in order to procure wood, being subject to physical damage (Padonou et al., 2022). Children too help their moms gather firewood or help collect firewood themselves and consequently are not allowed to attend school. Further, gathering wood by refugees can result in deforestation, environmental deterioration, and hostilities due to the competition for scarce resources.

Solar-based cooking has enormous potential to face the need for clean cooking by reducing energy consumption and improving the

* Corresponding author.
E-mail address: s.tomassetti@univpm.it (S. Tomassetti).

https://doi.org/10.1016/j.esd.2024.101409
Received 10 November 2023; Received in revised form 16 January 2024; Accepted 29 January 2024
Available online 10 February 2024

Nomenclature

Latin symbols

A	Area (m^2)
A_a	Aperture area (m^2)
a_0^*	Intercept of the cooking power linear fitting (W)
$a_1{}^*$	Opposite value of the slope of the cooking power linear fitting (W/°C)
C	Concentration ratio
COR	Cooker-opto-thermal-ratio (°Cm^2/W)
F'	Heat exchange efficiency factor
F_1	1st figure of merit (°Cm^2/W)
F_2	2nd figure of merit
G	Global horizontal solar irradiance (W/m^2)
G_{bn}	Direct normal solar irradiance (W/m^2)
G_n	Global normal solar irradiance (W/m^2)
G_n^*	Global normal solar irradiance at a particular solar radiation condition (=1000 W/m^2)
$\dot{Q}^*$	Cooking power (W)
$\dot{Q}_{50}^*$	Cooking power for $\Delta T_{f,a}{}^* = 50$ °C (W)
T	Temperature (°C)
T_{amb}	Ambient temperature (°C)
U_L	Overall heat loss coefficient (W/m^2°C)

Greek symbols

α	Sun elevation angle (°)
α_0	Intercept of the thermal efficiency linear fitting
α_1	Opposite value of slope of the thermal efficiency linear fitting (W/m^2°C)
β_1	Angle of left side (primary) reflector panel from horizontal plane (°)
β_2	Angle of right side (secondary) reflector panel from horizontal plane (°)
Δt	Time interval (s)
Δt_i	i-th time interval (s)
ΔT_f	Difference between the final and the initial values of temperature of the fluid in interval Δt (°C)
$\Delta T_{f,a}$	Difference between the load and ambient temperatures (°C)
$\Delta T_{f,a}^*$	Difference between the load and ambient temperatures associated with heating load process under a reference solar irradiance G_n^* (°C)
$\Delta T_{f,i}$	Variation of temperature of load in the i-th time interval (°C)
η	Instantaneous efficiency
η_{avg}	Average thermal efficiency
η_0	Optical efficiency
η_0'	Corrected optical efficiency
θ	Angle between the inclined glass to the horizontal plane (°)
χ	Specific temperature difference (m^2 °C/W)
Ω	Load thermal capacitance (J/°C)

Subscripts

a	Absorber, Aperture
abs	Absorber
amb	Ambient
avg	Average
c	Cooking
exp	Experimental
f	Fluid
G1	Horizontal glass
G2	Inclined glass
gl	Glycerin
P1	Primary reflector panel
P2	Secondary reflector panel
stg	Stagnation
w	Water

Acronyms

ASAE	American Society of Agricultural Engineers
HWB	Hottel-Whillier-Bliss
NIP	Normal Incidence Pyrheliometer

environment and human health (Martin et al., 2014; Panwar et al., 2011). In this regard, Sanglard et al. (2023) recently proved the better environmental performances of this alternative method than those of conventional Western cooking methods through a comparative life cycle assessment.

The devices that allow the direct use of solar energy for cooking purposes are called solar cookers (Arunachala & Kundapur, 2020; Battocchio et al., 2021). They are commonly classified as tube, panel, box, and parabolic cookers, but some particular designs are difficult to classify in these categories. Box solar cookers are among the most widespread and used devices. They usually consist of a thermally insulated box having a transparent element on the top and reflective panels to direct sunlight into the cooking chamber (Tiwari & Yadav, 1986). Additionally, a well-designed solar box cooker performs effectively even under intermittent direct solar irradiance, strong wind, and low ambient temperatures if the mass of the loaded food is low to moderate (Funk & Larson, 1998). However, due to their relatively high cost and the need for medium-level skills and tools for their construction, box solar cookers are not the best option for solar cooking in contexts of emergencies.

In the last decade, various studies have investigated and proposed several improvements and alternative designs of solar cookers (Aquilanti et al., 2023; Folaranmi, 2013; Joshi & Jani, 2015; Mahavar et al., 2012; Mirdha & Dhariwal, 2008; Regattieri et al., 2016; Sitepu et al., 2017). Below is a brief overview of some of the main studies in literature regarding foldable, small-sized solar cookers built with inexpensive materials.

A box cooker that is compact in design and affordable was manufactured and tested by Mahavar et al. (2012). A lightweight multilayer thermal insulation (corrugated cardboard, polystyrene expanded, and newspaper) and a specially designed polymeric glaze were used to construct the prototype. In the tests under no-load conditions, the plate reached a maximum temperature of 144 °C. The figures of merit, F_1 and F_2, were equal to 0.116 °C m^2/W and 0.466, respectively, and met the standards set by the Bureau of Indian Standards. The initial cooking power at $\Delta T = 0$ °C and the opposite value of the standardized cooking power linear regression's slope (Funk, 2003) were 103.5 W and 1.474 W/°C, respectively, making it a small cooker with good thermal insulation.

Regattieri et al. (2016) proposed and tested a portable, easy-to-use solar cooker obtained from recycled cardboard packaging waste. It was integrated into a complete kitchen-set box and became a self-sufficient cooking system without the need for traditional energy sources. The study aimed to find the optimal shape and efficiency of the cooker, which can heat, cook, boil water and purify raw water for people in emergencies.

Mirdha & Dhariwal (2008) studied different designs of booster mirrors for box cookers for optimizing their thermal performance. The study resulted in the development of an efficient and user-friendly device. The new design outperformed a conventional box-type solar cooker. It could also prepare two meals daily and keep food warm in the evenings.

Folaranmi (2013) analyzed the performance of a double-glazed box cooker having a reflector. The prototype was constructed using locally available materials, compressed sawdust as insulation, and black-painted aluminum as absorber plate. The device had a double-glazed lid cover that allowed the penetration of the solar radiation into the absorber surface and reduced convection heat loss. From the tests' results, F_1, F_2, and cooking power were determined to be 0.11 °C m^2/W, 0.31, and 23.95 W, respectively.

Sitepu et al. (2017) conducted tests to characterize a solar box cooker (area equal to100 cm × 100 cm and a height equal to 40 cm) equipped with two booster reflector panels. The results showed that a maximum temperature of 117 °C was reached in a test without load and the cooker was able to boil 2 kg and 4 kg of water in 165 min and 197 min, respectively. Additionally, the efficiency of the cooker was estimated to be 46.30 %.

Aquilanti et al. (2023) developed and tested a new type of solar cooker with a Newton prism-shaped cooking chamber. It was made using inexpensive materials and designed to be simple to build, use, and transport. It had a manual tracking system and wheels at the base to follow the sun's movements. During the outdoor experiments, two identical cookers, one with and one without wind protection, were analyzed. The authors performed tests without load and with water and glycerin as loads. From the tests without load, it was found that the cooker had good thermal performance, with the air inside the cooking chamber reaching 137 °C. The shielded device brought 2 kg of water to the boiling point and 2 kg of glycerin from 40 °C to 110 °C in 2 h and 2.84 h, respectively.

In the humanitarian aid's context, the use of solar cookers by people in need had preliminary to face the problems connected to the delivery of such goods, and so, in general terms, the humanitarian logistics issue. Humanitarian logistics is "the process of planning, implementing and controlling the efficient, cost-effective flow and storage of goods and materials as well as related information from the point of origin to the point of consumption for the purpose of alleviating the suffering of vulnerable people." (Thomas & Kopczak, 2005). Humanitarian logistics covers different actions, among which transportation, storage, handling, and distribution that need to be developed and optimized to improve the performance of humanitarian operations (da Costa et al., 2012). In most of these actions, the capacity of vehicles and facilities is considered a constraint. Thus, the volume of solar cookers became a major feature for their use in emergency context (Safeer et al., 2014). However, this feature is not usually considered of primary importance in the literature on solar ovens.

Recently, a prototype of a foldable solar cooker for cooking in the humanitarian context without electricity, wood, and fossil fuels has been designed by Matteo Muccioli, co-author of this study. Moreover, some authors of this work have applied for a patent on the prototype; currently, its status is pending patent approval (Paciarotti et al., 2022). The prototype was designed to be foldable and portable, using easily accessible and inexpensive materials for construction. The device is characterized by a trapezoidal cooking chamber with the bottom and three sides consisting of wood panels, while the top and the other side consist of glass layers. The glass layers can be easily removed for loading the cooking chamber. Moreover, it comprises reflector panels on the sides of which inclination can be adjusted to maximize the concentrated solar radiation. The reflector panels, cooking chamber, and tempered glass of the prototype can be stacked and easily reassembled for transport to refugee camps and other humanitarian settings during emergencies and crises. It is possible to disassemble the box in its whole, and each of its components may be conveniently stacked to be stored or carried (closed size about 60 × 40 × 7 cm). Therefore, the solar cooker is characterized by excellent transportability, one of the primary needs in these contexts. Additionally, the prototype was capable of bringing 0.5 l of water at boiling point temperature in 80 min, reaching a maximum temperature of 130 °C when tested with glycerin as load under a normal global solar irradiance of 900 W/m^2. However, the prototype lacked adequate experimental testing to characterize its performance fully and required further investigation. Thus, this study aims to evaluate the device's thermal and cooking performances based on various parameters by conducting tests without and with load (water, glycerin, and food) on different days. In addition, the effect of different enclosures for the cooking pot on the device performance was evaluated. Furthermore, the study includes a detailed account of the solar cooker's design, construction, and usage.

The research paper is organized in seven sections. The Transportability for "humanitarian energy" section describes the need to ensure the cooking devices' transportability in the humanitarian context. The Design and details of the prototype section presents the solar cooker's design and main features, together with its optical analysis. The Manufacturing and cost analysis section describes the manufacturing process and cost analysis of materials. The Methods section includes the methods to carry out the tests and analyze the parameters. The Experimental results section shows the experimental results of the study and a discussion of them. Finally, the Conclusions section summarizes the overall findings of the study.

Transportability for "humanitarian energy"

The capacity of commodities, products, or objects to be efficiently transferred from one area to another without damage or loss is referred to as their transportability. This ability ensures that the goods' original integrity and quality are maintained during the process of transportation and that the transport phase is easy and cost-efficient. It is essential to ensure the transportability of things in various industries, such as manufacturing, logistics, and supply chain management, to preserve the effectiveness of costs, satisfaction with consumers, and overall efficiency in operation (Christopher, 2016; Mangan et al., 2008). In particular, transportability plays a vital role in the domain of humanitarian logistics as it ensures the efficient and prompt distribution of vital products and services to populations impacted by natural calamities, wars, or other humanitarian emergencies (Kovács & Spens, 2007; Tatham & Christopher, 2018). The notion of transportability has significant importance in facilitating the effective delivery of help and relief goods to individuals in need, irrespective of the adverse and sometimes volatile circumstances prevalent in disaster-stricken regions. By prioritizing the aspect of transportability, humanitarian organizations have the potential to improve their logistical capacities and streamline their activities to deliver crucial aid and assistance to people in need.

Over the past few years, some international humanitarian organizations have moved toward product transportability by publishing catalogs of kits (Berger & Garyfalakis, 2013). An illustration of this can be seen in the United Nations High Commissioner for Refugees Core Relief Items Catalogue (United Nations High Commissioner for Refugees (UNHCR), 2012), the Catalogue and Brochure of Disaster Emergency Logistics System for ASEAN Relief Items (ASEAN Coordinating Centre for Humanitarian Assistance on Disaster Management, 2017), and the International Federation of Red Cross and Red Crescent Societies standard products catalogue (International Federation of Red Cross and Red Crescent Societies (IFRC), 2017). The kits are mainly light, transportable, and compact. Also, they can serve as facilitators in the execution of supply chain tasks pertaining to the handling, transportation, and storage of materials.

In light of the frequently compromised transportation scenarios and infrastructure that arise during humanitarian emergencies, Savonen et al. (2018) developed the concept of a transportable 3-D printer specifically engineered to facilitate deployment within crisis zones. This entails possessing portability that enables it to accept various modes of transportation and exhibiting durability that prevents any harm throughout the transit process.

From a logistical point of view, the strategic importance of a portable item in a humanitarian context also emerges from the Relief Material Classification proposed by Shao et al. (2020). The authors introduced

Table 1
Components of the solar cooker. The component symbols and names refer to the labels shown in Fig. 1.

Component symbol	Component name	Materials	Quantity
C_1	Side panels	MDF wood	2
C_2	Bottom-side panel	MDF wood	1
C_3	Left-side panel	MDF wood	1
C_4	Transparent glass layer	Tempered glass	2
C_5	Reflector panels	PMMA	2
C_6	Left-side panel supporter	MDF wood	1
C_7	Left-side reflector panel supporter	MDF wood	1
C_8	Right-side reflector panel supporter	MDF wood	1
C_9	Hinges with 3 holes	Steel metal	2

the demand checklist for various catastrophes and natural situations and the supply categories aligned with the Chinese reserve system. Within this list, it is possible to notice the presence of some foldable items such as foldable beds, tables and chairs, field clinic beds, stretchers, and hospital beds. The inclusion of such portable items provides benefits in their stocking, handling, and transportation.

Other examples of foldable items for humanitarian context are reported in the humanitarian shelter field. The frequency and the destructive impact of catastrophes have led to a significant growth in the demand for alternative temporary shelters for populations affected by such events in recent years. Transportability and easiness of storage are two of the most important criteria that should be taken into account while designing shelters for temporary use (Cerrahoğlu & Maden, 2022). During the pre-disaster phase, it is crucial to store shelters in a manner that ensures their preservation and minimizes spatial requirements. Given the uncertainty surrounding the number of shelters required in post-disaster, it is imperative to provide a sufficient availability of such facilities. Subsequently, in the event of a calamity, expeditious availability of shelters near the intended area is the highest priority. Hence, in light of the transit vehicles' carrying capacity, it is imperative that the shelters are of small dimensions and appropriately sized. They should also possess a lightweight construction. Through the implementation of this approach, a greater number of shelters may be efficiently transported and promptly provided simultaneously. Literature analysis reveals that a significant proportion of the temporary shelters currently in use encounter significant challenges related to transportation and storage (Cerrahoğlu & Maden, 2022). As an answer to this issue, many authors designed, tested, and proposed innovative shelters that occupy little space for transportation, enabling convenient transportation to any desired destination in its closed form. Examples are the studies of Costa et al. (2022), Popescu et al. (2021), and Mercader-Moyano & Porras-Pereira (2023).

Transportability is also an emerging need for "humanitarian energy", which is the comprehensive framework encompassing institutions, programs, policies, global initiatives, and activities that employ diverse sustainable and fossil fuel energy sources within the specific contexts of humanitarian operations. Humanitarian energy's primary objective is to address the energy requirements of individuals residing in camps and urban environments, as well as self-settled refugees, internally displaced persons, and host communities (Rosenberg-Jansen, 2019). Transportable and foldable solutions for energy supply in humanitarian contexts have been developed and successfully implemented, as shown in different studies (Franceschi et al., 2014; Noyes & Jones, 2019). Literature on humanitarian energy suggests different energy use categories (Noyes & Jones, 2019): household cooking, household electricity, energy access for enterprises, energy access for community facilities (e.g., refugee governance centers and schools), and energy access for institutional users (humanitarian agencies or NGOs). The present paper is part of the first category, i.e., energy use for household cooking purposes. The transportability of a product is mostly determined by its dimensions, mass, and shape (Noyes & Jones, 2019) and the foldable solar cooker fits well with all these requirements, as shown in the following sections.

Design and details of the prototype

The solar cooker is composed of the different parts listed in Table 1 and shown in Fig. 1a. Fig. 1b shows 2D drawing views of the cooker.

The cooker comprises a trapezoidal cooking chamber with a volume of 0.0218 m^3, covered with single glass layers (component C_4) of 340 mm length, 250 mm width, and 2 mm thickness on the top and inclined surfaces, while the remaining surfaces are covered with wooden panels (C_1, C_2, and C_3). The side panels C_1 are right trapezoidal prisms with bases of 455 mm and 315 mm, height of 210 mm, and thickness of 10 mm. The rectangular panels C_2 (570 mm × 400 mm × 10 mm) and C_3 (450 mm × 340 mm × 10 mm) are placed at the base and left side, respectively. The left-side panel (C_3) is supported by a wooden strip (C_6) with a length 340 mm, width 50 mm, and thickness 10 mm. A black pot can be directly used as a cooking device inside the cooking chamber. However, for higher cooking performance, it is recommended to use a black pot within a transparent enclosure, e.g., a glass bowl or a plastic bag, as a cooking device. Additionally, the prototype incorporates two equal-sized reflector panels (C_5) (length of 500 mm, width of 300 mm, and thickness of 1 mm) made of aluminum reflectors to reflect the solar radiation inside the cooking chamber. As shown in Fig. 1a, one reflector is placed on the left side, i.e., back side of the cooker, while the second is connected to the base of the cooking chamber on the right side, i.e., on the front side of the cooker. A wooden rod with a dimeter of 20 mm (C_7) and a wooden wedge (C_8) allow changing the inclination of the right and left-side reflector panels, respectively, for maximizing the quantity of solar radiation reflected into the cooking chamber. The components C_9 are hinges with 3 holes on each side.

Fig. 2 illustrates the schematic diagram of the prototype and the illustration of the four area elements considered for calculating the aperture area (A_a). The aperture area is defined as the projection onto a plane perpendicular to the sun's rays of the area delimited by the prototype's outer edges. During the tests conducted on various days, the angles between the left side (primary) and right side (secondary) reflector panels and the horizontal plane (β_1 and β_2, respectively), as well as the sun elevation angle (α), showed minimal variation. Therefore, the average values of $\beta_1 = 94^o$, $\beta_2 = 35^o$, and $\alpha = 60^o$ were used to calculate the aperture area. The aperture area of the prototype was calculated as follows:

$$A_a = A_{a,P1} + A_{a,G1} + A_{a,G2} + A_{a,P2} \quad (1)$$

where $A_{a,P1}$, $A_{a,G1}$, $A_{a,G2}$ and $A_{a,P2}$ are the aperture area of the elements associated with the primary reflector panel, horizontal glass, inclined glass, and secondary reflector panel, respectively. As shown in Fig. 2, their values can be calculated as follows:

$$A_{a,P1} = A_{P1} sin\,(180 - \beta_1 - \alpha) \quad (2)$$

$$A_{a,G1} = A_{G1} sin(\alpha) \quad (3)$$

$$A_{a,G2} = A_{G2} sin(180 - \theta - \alpha) \quad (4)$$

$$A_{a,P2} = A_{P2} sin\,(\alpha - \beta_1) \quad (5)$$

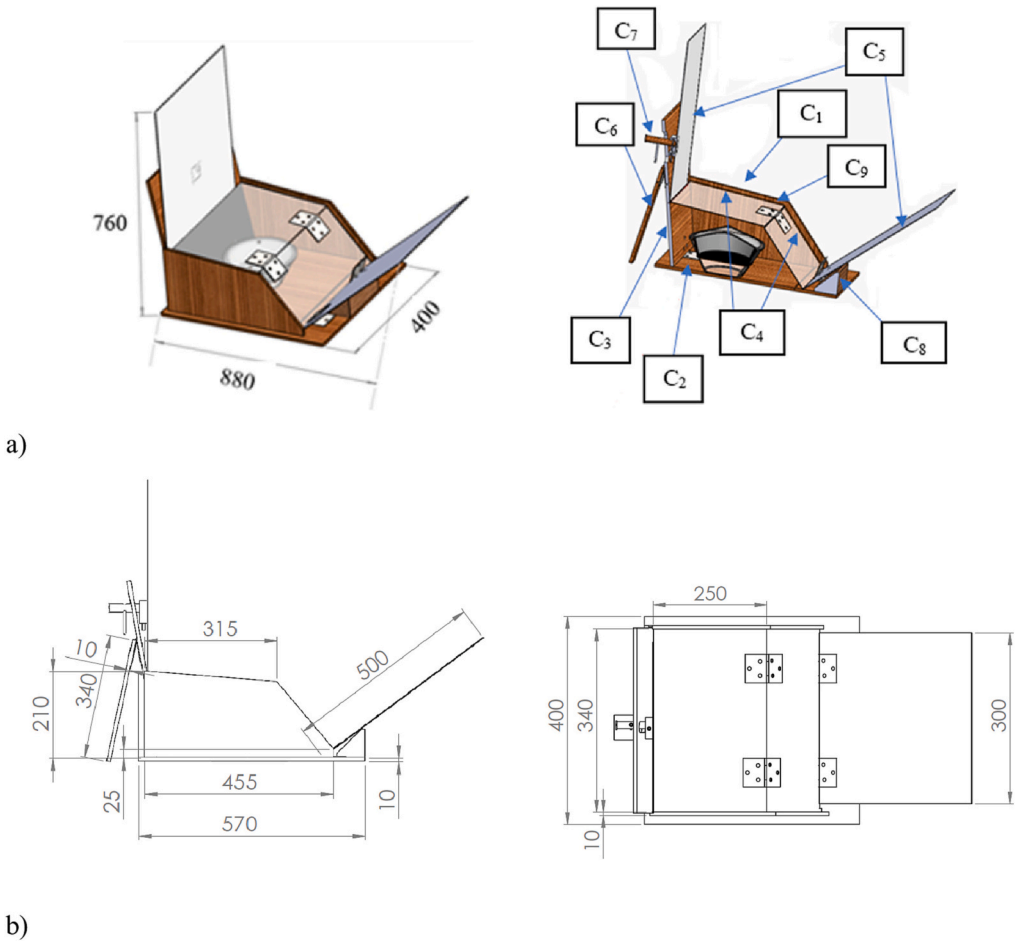

Fig. 1. Solar cooker design: a) 3D views, b) side and top views. The dimensions are in mm. The reported labels refer to the component symbols of Table 1.

where $A_{P1} = A_{P2} = 0.15\ m^2$, $A_{G1} = A_{G2} = 0.085\ m^2$ and θ is an angle between the inclined glass to the horizontal plane which is equal to 40°. Thus, the total aperture area is equal to 0.286 m^2.

Manufacturing and cost analysis

The fabrication process involved cutting two identical trapezoidal (component C_1), and rectangular wooden panels (C_2 and C_3), as well as two rectangular tempered glass layers (C_4) and reflector panels (C_5). These components were assembled as shown in Fig. 1. The bottom panel (C_2) was attached to the left panel (C_3) using a hinge (C_9), allowing for easy folding of the device. The cooking chamber was constructed by placing the trapezoidal wooden panels (C_1) vertically at the front and back of the bottom panel (C_2) and covering the space with the two tempered glass pieces (C_4) joined with a hinge (C_9). The left-side wooden panel supporter (C_6) was attached to the back of the left wooden panel (C_3) using a hinge (C_9) to resist wind loads and align the left reflector panel (C_5) with the sun's position. The left-side panel (C_3) was also drilled at the top to place the left-side reflector panel supporter (C_7).

The folded prototype shown in Fig. 3 has dimensions of 600 mm × 400 mm × 70 mm and has a net mass of 7 kg. Based on the UNE-EN 13698–1 standard for Euro-single pallet size (U. E. 13698-1 Standard, 2022), a pallet has a dimension of 800 mm × 1200 mm × 144 mm, can hold 1500 kg, and has a maximum height limit of 2200 mm for a load. Considering all these constraints, a Euro-pallet can transport 124 device pieces.

Table 2 presents the cost of the components of the current solar cooker design. Its total cost was equal to 39 euros, i.e., about 42 US dollars considering an exchange rate of 1.09 US dollars/euros (January 2024). Since the proposed device requires minimal maintenance, it can be considered a practical and cost-effective option for solar cooking. However, the costs of the black pot, glass enclosure (glass bowl), and plastic enclosure (plastic bag) used during the tests were not considered in the cost analysis. The black pot, glass bowl, and plastic bag cost 5, 41, and 2 euros, respectively.

Methods

Experimental setup

Tests were performed using the black stainless-steel pot enclosed with a glass bowl with a glass lid or a plastic bag, as depicted in Fig. 4. Some tests were performed with an unloaded pot and others with a load. The black pot had a mass of 0.48 kg. Its diameter, height, and thickness were 200 mm, 130 mm, and 2 mm, respectively. The tempered glass bowl with the glass lid had a mass of 1.3 kg. Its upper external diameter, lower external diameter, and thickness were 230 mm, 100 mm, and 3 mm, respectively. The plastic bag had dimensions of 550 mm × 600 mm.

T-type thermocouples were adopted for measuring ambient temperature (T_{amb}), pot's bottom surface (absorber) temperature for the test without load (T_{abs}), and fluid's medium level temperature for the tests with load (T_f). The uncertainty for the measured temperatures is ±1 °C. The direct normal solar irradiance (G_{bn}) was measured using an Eppley normal incidence pyrheliometer (NIP) installed on a solar tracker. The NIP has a ± 0.5 % linear relationship between 0 W/m^2 and 1400 W/m^2, a 1 s time response, a 1 % temperature dependence from −20 °C to 40 °C, and a calibration uncertainty of about 1 %. A pyranometer SR30-

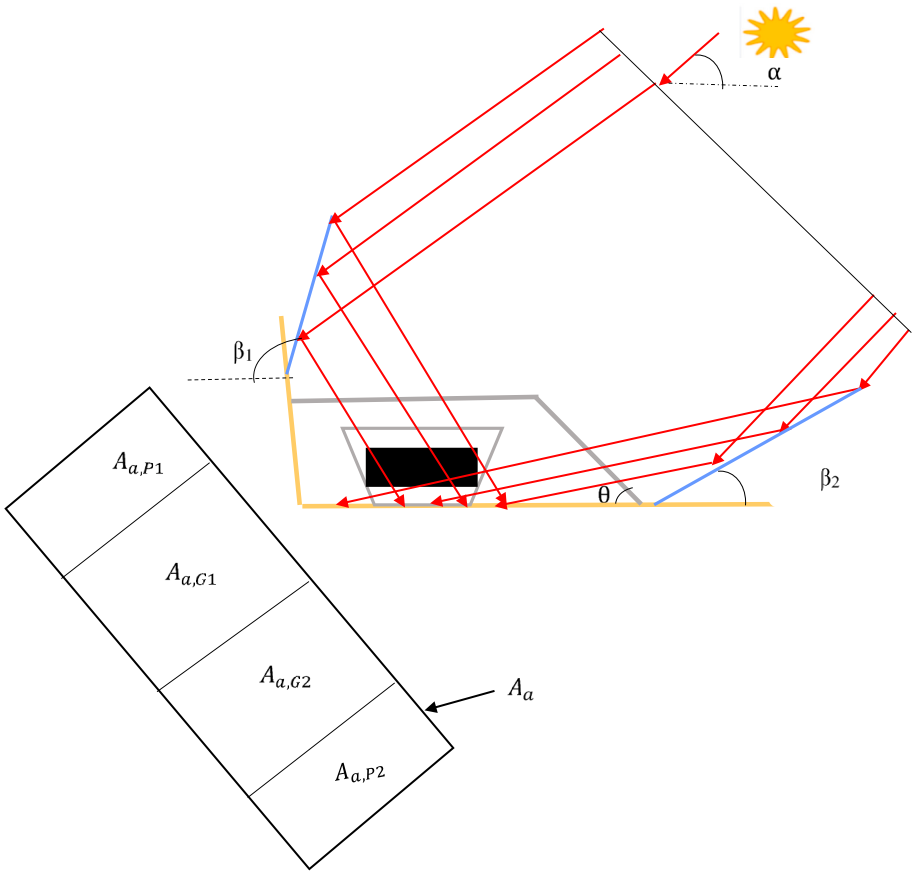

Fig. 2. Schematic diagram of the solar cooker defining its aperture area.

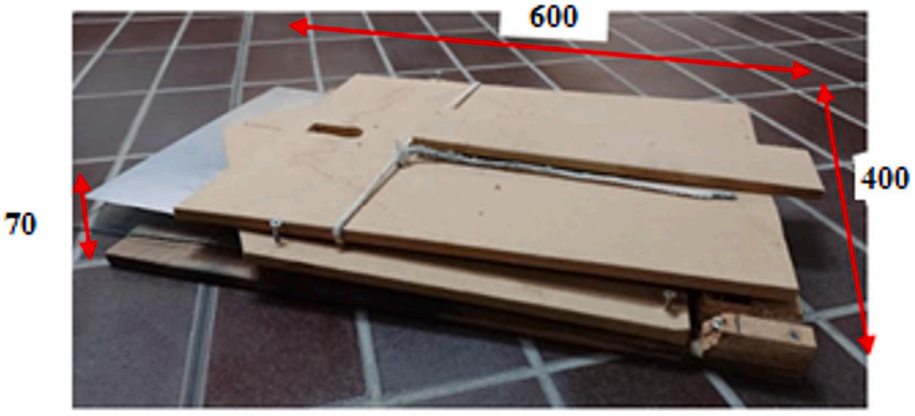

Fig. 3. Solar cooker folded. The dimensions are in mm.

Table 2
Summary of the components' costs.

Item	Cost (euros)
Aluminum Reflector Panels	18
MDF Wood	4
Steel hinges	3
Tempered glasses	6
Miscellaneous	8
Total	39

M2-D1 having a 3.0 % linearity between 0 and 4000 W/m^2 and a calibration uncertainty of 1.5 % was put horizontally in the proximity of the prototype to measure the global horizontal solar irradiance (G). The global normal solar irradiance (G_n) was determined through the Liu-Jordan-isotropic-sky model (Duffie & Beckman, 2013) and an albedo of 0.2, as explained elsewhere (Aquilanti et al., 2023; Ruivo et al., 2022). Data were collected and analyzed using a Pico-Technology TC-08 data logger with eight inputs and the Pico-Log data gathering tool, which provided real-time visualization and data export for post-testing analysis. The measuring system used in this study, which can test one or two cookers at the same time, is schematized in Fig. 5.

Fig. 4. Cooking pot with: a) a glass enclosure and b) a plastic enclosure.

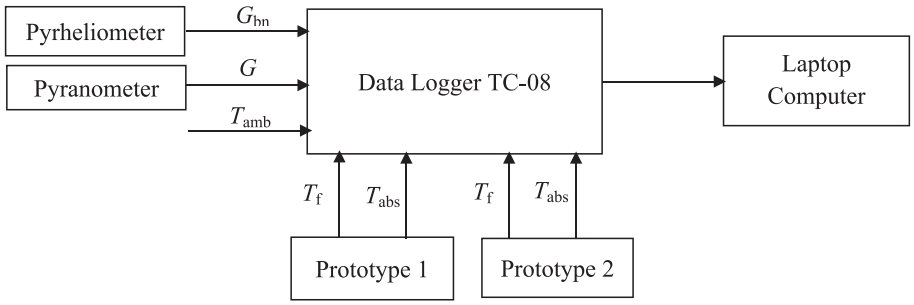

Fig. 5. Measuring system used during the tests. G_{bn}, direct normal solar irradiance; G, global horizontal solar irradiance; T_{amb}, ambient temperature; T_f, fluid temperature; T_{abs}, absorber temperature.

Experimental tests

Experiments were conducted on the roof of the DIISM building of Marche Polytechnic University, Italy, located at a latitude of 43.5871° N and a longitude of 13.5149° E. Tests were conducted over two consecutive years: a single prototype was used in 2022, while two identical prototypes (referred to as pro1 and pro2 below) were tested in parallel in 2023. The stagnation temperature value was determined through experiments performed without load. Water was used as the test fluid for the experiments due to its widespread use and well-known physical and chemical characteristics. However, water may not always be appropriate when the cooker is meant to work above its boiling temperature. As a result, glycerin was used as an additional fluid to analyze the solar cooker at higher temperatures. Throughout the tests, the ambient temperature and direct normal solar irradiance were recorded within a range of 24 °C to 35 °C and 800 W/m^2 to 1000 W/m^2, respectively. The cooking parameters were determined within a range of 40 °C to 90 °C for the water load test and 40 °C to 105 °C for the glycerin load test, The specific heat capacities of water and glycerin considered in the calculations were 4182 J/ (kg °C) and 3014 J/ (kg °C), respectively. The orientation and angles of the cooker's reflectors were adjusted every 15 min by observing the reflected radiation that reached the black cooking pot. Finally, cooking tests were done to find the ability of the proposed cooking appliance in actual cooking. The time required to bring the tested food (i.e., tomatoes, rice, and potatoes) to the cooking temperature was derived from the food temperature recorded during the tests.

Performance parameter for solar cooker testing without load

The tests without loaded pot were used to achieve the solar cookers' stagnation condition. In a stagnation test, the black pot (absorber) temperature (T_{abs}) rises initially and reaches the maximum temperature over time. In the stagnation condition, the 1st figure of merit F_1 can be calculated as follows (Mullick et al., 1987):

$$F_1 = \frac{\eta_0}{U_L} = \frac{T_{stg} - T_{amb}}{G_n} \tag{6}$$

where η_0 and U_L are the optical efficiency and the overall heat transfer coefficient, respectively. The temperature T_{stg} is the stagnation temperature. It corresponds to the maximum temperature reached at the bottom surface inside the black pot (T_{abs}). Instead, T_{amb} and G_n are the ambient temperature and global normal solar irradiance, respectively.

Performance parameters for solar cooker testing with load

For the tests with load, the 2nd figure of merit (F_2) is defined as (Mullick et al., 1987):

Table 3
Summary of the results without load.

Parameters	Glass enclosure			Plastic bag enclosure		
Testing days	16/5/2022	19/5/2022	1/6/2022	2/8/2023	3/8/2023	8/8/2023 pro2
Starting local clock time (hh:mm)	9:40	9:44	9:31	9:40	9:07	9:57
Ending local clock time (hh:mm)	13:52	15:14	14:37	12:04	11:33	12:45
G_n (W/m^2)	935.13	1091.02	984.56	962.03	1065.25	1074.34
T_{amb} (°C)	29.52	24.66	27.66	28.80	33.23	26.79
T_{abs} (°C)	149.38	137.24	136.61	130.00	122.98	133.79
F_1 (°C m^2/W)	0.128	0.103	0.111	0.105	0.084	0.100

$$F_2 = \frac{F_1 \Omega}{A_a \Delta t} ln \left[\frac{1 - \frac{1}{F_1}\left(T_{f1} - T_{amb,avg}\right) \Big/ G_n}{1 - \frac{1}{F_1}\left(T_{f2} - T_{amb,avg}\right) \Big/ G_n} \right] \quad (7)$$

where Ω is the thermal heat capacity of the fluid, calculated as the product of fluid mass and the specific heat of the fluid. The T_{f1} and T_{f2} variables are initial and final values of temperature of the fluid in a time interval Δt, and $T_{amb,avg}$ is the average ambient temperature in the same time interval. The average overall efficiency for Δt where the temperature of the fluid changes from T_{f1} to T_{f2} is (Mullick et al., 1987):

$$\eta_{avg} = \Omega \frac{\Delta T_f}{G_n A_a \Delta t} \quad (8)$$

where $\Delta T_f = T_{f2} - T_{f1}$. In particular, T_{f1} and T_{f2} are equal to 40 °C and 90 °C, respectively, for the water load tests and 40 °C and 105 °C, respectively, for the glycerin load tests.

Since the inaccuracy of the ASAE S580.1 Standard (Funk, 2003) procedure to calculate the standardized cooking power (Ruivo et al., 2022), the procedure to derive cooking power $\left(\dot{Q}^*\right)$ at any solar irradiance recently adopted by Ruivo et al. (2022) was also used in this work. Its base is the Hottel-Whillier-Bliss (HWB) formulation and has the following expression:

$$\dot{Q}^* = a_0{}^* - a_1{}^* \Delta T_{f,a}{}^* \quad (9)$$

where $a_0{}^*$ and $a_1{}^*$ are the linear regression's coefficients and $\Delta T_{f,a}{}^*$ is the difference between the load and ambient temperatures ($\Delta T_{f,a}$) associated to the heating process of the load under the reference solar irradiance G_n^*. The following relationship can be derived:

$$\Delta T_{f,a}{}^* = \Delta T_{f,a} \frac{G_n^*}{G_{n,exp}} \quad (10)$$

where G_n^* is the global normal solar irradiance at a particular solar radiation condition. In present study, the value of clear sky condition G_n^*=1000 W/m^2 is considered instead of using the value suggested by the ASAE 580.1 Standard (700 W/m^2). The variable $G_{n,exp}$ is the global normal solar irradiance at the conditions of the experiment.

To calculate the coefficients of Eq. (9), the power can be firstly calculated for each 5-min interval as follows:

$$\dot{Q}_i^* = \Omega \frac{\Delta T_{f,i}}{\Delta t_i} \frac{G_n^*}{G_{n,exp,i}} \quad (11)$$

where $\Delta T_{f,i}$ and $G_{n,exp,i}$ are the variation of the load temperature and the global normal solar irradiance in the i-th time interval, respectively. The

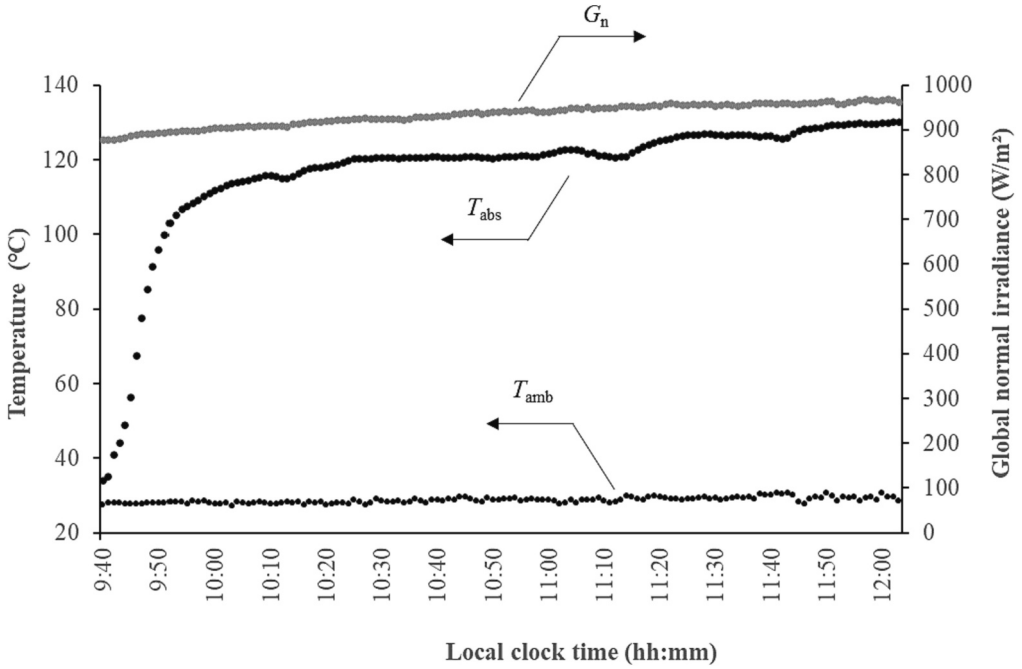

Fig. 6. Test performed without load using a plastic bag on 2/8/2023 pro2.

Table 4
Summary of the results for water load tests (the parameters and the arithmetic average values were calculated in the temperature range from 40 °C to 90 °C).

Parameters	Glass enclosure										Plastic bag enclosure			
Testing days	13/6/2022	14/6/2022	13/7/2022 test1	13/7/2022 test2	26/7/2022 test1	26/7/2022 test2	29/7/2022	3/7/2023 pro1	3/7/2023 pro2	21//7/2023	6/7/2023	17/7/2023 pro1	19/7/2023 pro2	8/8/2023 pro1
$G_{n,avg}$ (W/m^2)	854.21	930.88	970.04	1050.31	901.07	930.44	907.20	1005.20	1005.29	928.03	985.65	911.06	889.70	1062.75
$T_{amb,\ avg}$ (°C)	29.96	26.93	27.53	30.89	30.91	31.85	29.63	29.87	29.83	34.84	28.24	34.82	32.17	25.58
Starting local clock time (hh:mm)	9:52	10:14	10:07	12:09	10:15	12:40	9:55	10:21	10:16	10:41	10:35	10:38	10:28	10:47
Ending local clock time (hh:mm)	11:43	12:18	11:50	13:43	12:17	14:46	12:02	12:11	12:07	12:41	12:53	12:41	13:14	12:37
Δt (min)	110.00	123.00	102.00	93.00	121.00	126.00	127.00	110.00	111.00	120.00	131.00	122.00	166.00	110.00
η_{avg}	0.13	0.10	0.12	0.11	0.10	0.10	0.10	0.15	0.15	0.10	0.13	0.10	0.08	0.16
F_2	0.21	0.16	0.19	0.16	0.16	0.15	0.16	0.24	0.24	0.15	0.27	0.15	0.12	0.11
$\dot{Q}_{50}^{*}$ (W)	34.7	27.5	27.5	23.2	25.5	24.0	27.4	25.4	23.0	21.8	21.5	19.5	18.2	24.5
$F' U_L/C$ (W/m^2 °C)	3.29	1.80	2.43	2.53	2.18	2.62	2.26	1.67	3.29	2.33	2.60	3.49	3.25	1.78
$F'\eta$ (W/m^2 °C)	0.28	0.18	0.22	0.21	0.19	0.21	0.20	0.17	0.23	0.19	0.20	0.24	0.23	0.18
COR (°C m^2/W)	0.086	0.099	0.091	0.081	0.089	0.081	0.090	0.103	0.071	0.081	0.078	0.070	0.069	0.098

time interval Δt_i is equal to 300 s. The calculated $\dot{Q}_i^{*}$ are plotted as a function of corresponding $\Delta T_{f,a,i}{}^{*}$. The values of $a_0{}^{*}$, and $a_1{}^{*}$ are obtained from the linear regression of the plotted data.

The power at 50 °C temperature difference between load and air ($\dot{Q}_{50}^{*}$) can be calculated from Eq. (9) considering $\Delta T_{f,a,i}^{*} = 50$ °C.

According to the HWB formulation usually applied when reporting the performance of solar collectors used to heat up a water flow, the instantaneous efficiency of a solar cooker in the process of heating up a certain mass of water or another fluid can be mathematically expressed as (Khalifa et al., 1985; Ruivo et al., 2022):

$$\eta = F'\eta_o - \left(\frac{F'U_L}{C}\right)\frac{T_f - T_{amb}}{G_n} = \alpha_0 - \alpha_1\chi \tag{12}$$

where F' corresponds to the heat exchange efficiency factor, C is the concentration ratio, and $\chi = (T_f - T_{amb})/G_n$. The coefficients α_0 and α_1 can be determined from the plot of points (η,χ) calculated in 5 min intervals. In fact, α_0 and α_1 are the intercept value and the opposite value of the thermal efficiency linear fitting's slope, respectively. The opto-thermal ratio of the cooker (COR) can be calculated using the regression coefficients and is given numerically as (Khalifa et al., 1985; Ruivo et al., 2022):

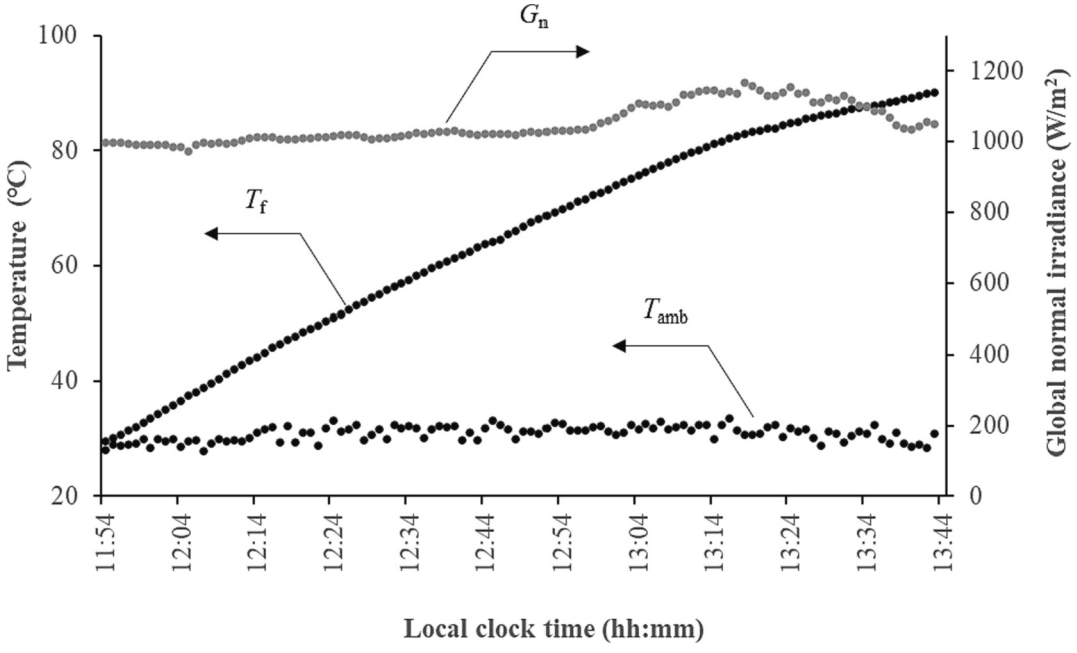

Fig. 7. Test performed with water load with a glass enclosure on 13/7/2022 test2.

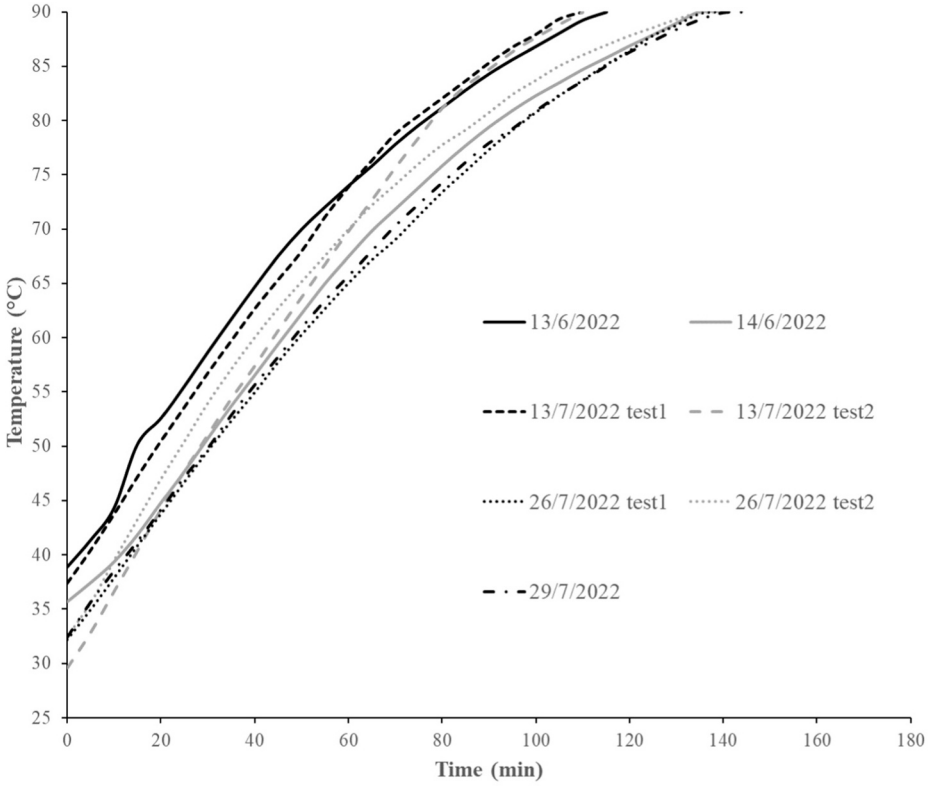

a)

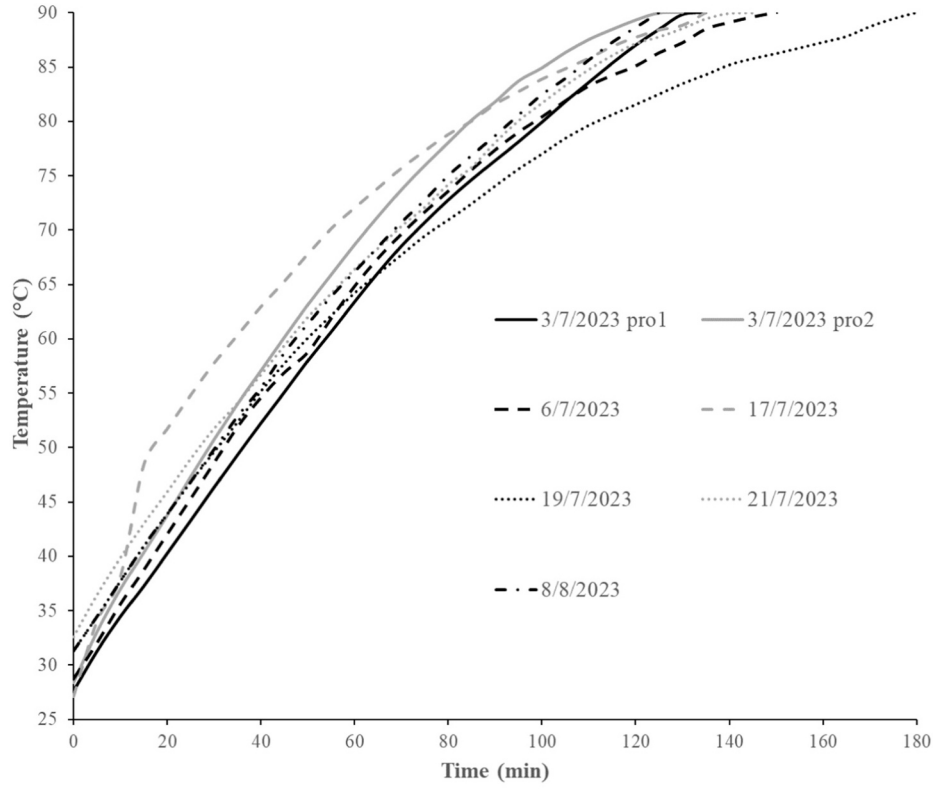

b)

Fig. 8. Time evolutions of load temperature until 90 °C for all water load tests: a) 2022 tests and b) 2023 tests. Details for the tests are reported in Table 4.

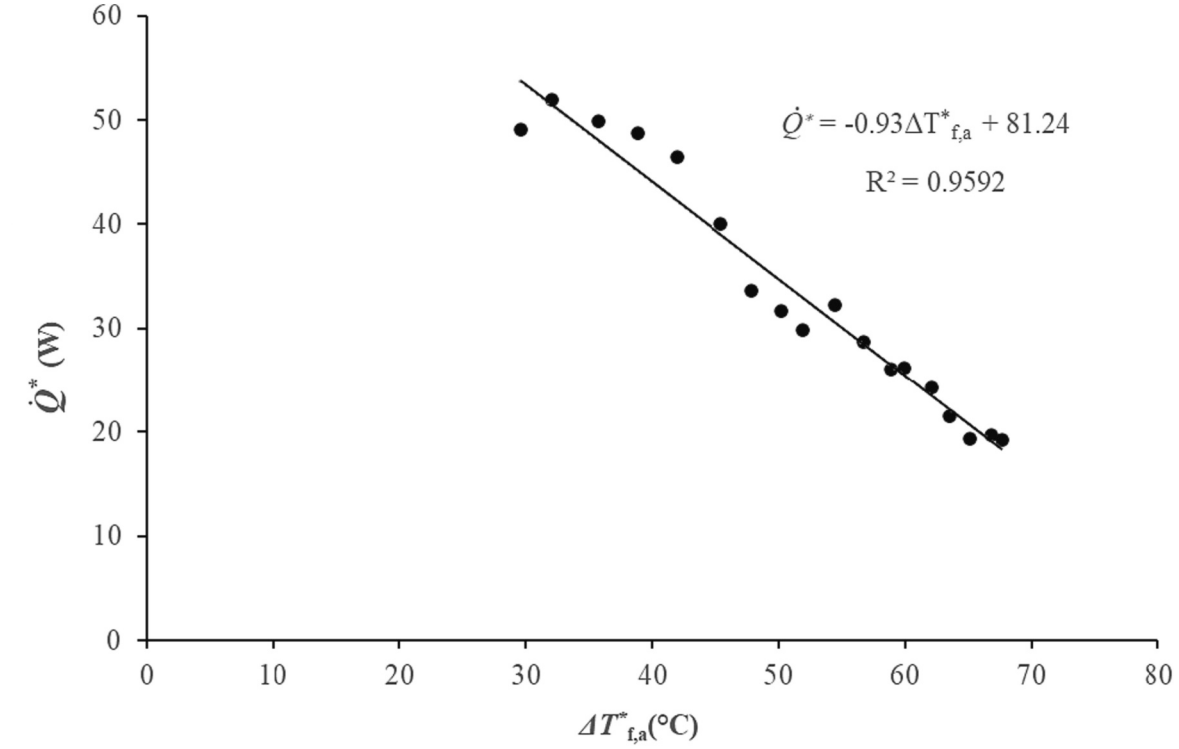

a)

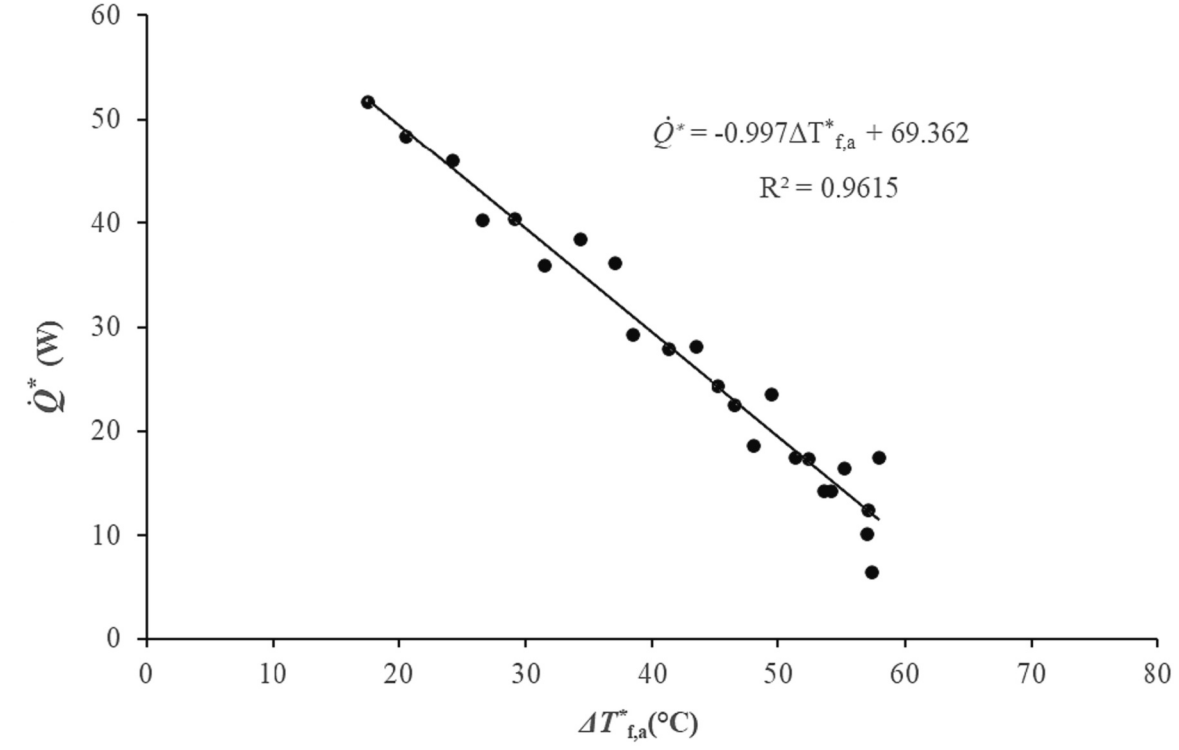

b)

Fig. 9. Coking power curve as a function of temperature difference for the tests performed with water: a) on 13/6/2022 with glass enclosure and b) on 17/7/2023 pro1 with plastic bag.

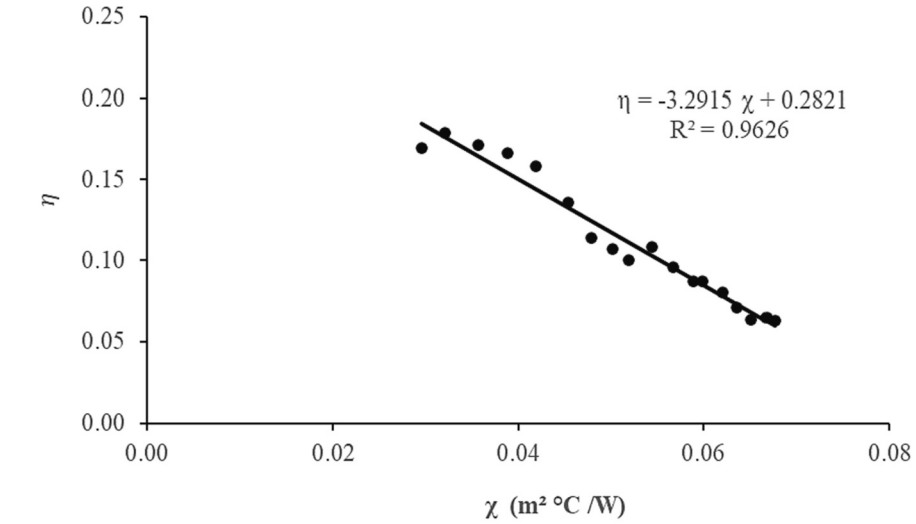

a)

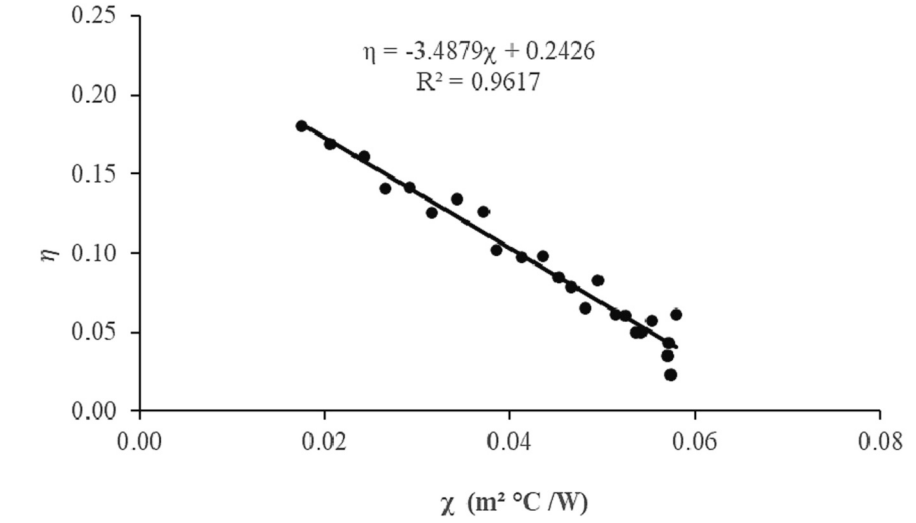

b)

Fig. 10. Efficiency of the cookers for the tests performed with water: a) on 13/6/2022 with glass enclosure and b) on 17/7/2023 pro1 with plastic bag.

$$COR = \frac{\alpha_0}{\alpha_1} = \frac{\eta_o C}{U_L} \quad (13)$$

Experimental results

Test without load

Five tests without a load were performed under various conditions, in three of which the pot was enclosed with a glass bowl, and in the remaining two, it was enclosed with a plastic bag. The obtained results are reported in Table 3. The maximum temperature of the black pot (T_{abs}), its associated global normal irradiance (G_n), and ambient temperature (T_{amb}) were determined from the measured data. Two identical prototypes were used parallelly in some 2023 tests, referred to as pro1 and pro2 below.

These parameters are also shown in Fig. 6, depicting the test performed on 2/8/2023. In the tests of 16/5/2022 performed using the glass enclosure and 8/8/2023 pro2 carried out using a plastic bag, the maximum temperature reached by the black pot were 149.38 °C and 133.79 °C, respectively. These maximum temperatures correspond to G_n of 935.13 W/m^2 and T_{amb} of 29.52 °C during the test of 16/5/2022, while G_n of 1074 W/m^2 and T_{amb} of 26.79 °C during the 8/8/2023 pro2 test. The mean values of F_1 for the three tests with the glass enclosure and the two tests with the plastic bag were equal to 0.114 °C m^2/W and 0.096 °C m^2/W, respectively. This value was used to calculate F_2 for the load tests.

Tests with water

The results of twelve water load tests are presented in Table 4. Ten tests with a glass enclosure and two with a plastic bag enclosure were performed using 1 kg of water. Additionally, Table 4 indicates that two tests were conducted on some days. The first and second tests are referred to as test1 and test2, respectively. The parameter values and the arithmetic average values were calculated between 40 °C to 90 °C.

During the 13/7/2022 test2, the temperatures and solar irradiance

Table 5
Summary of the results for glycerin load tests (the parameters and the arithmetic average values were calculated between 40 °C and 105 °C).

Parameters	Glass enclosure				Plastic bag enclosure		
Testing days	21/6/2022	29/6/2022	19/7/2022	20/7/2022	17/7/2023 pro2	2/8/2023	3/8/2023
$G_{n,avg}$ (W/m^2)	839.09	898.66	980.09	955.05	905.90	934.73	1058.28
$T_{amb,\ avg}$ (°C)	31.61	28.65	28.09	29.31	34.88	28.72	30.09
Starting local clock time (hh:mm)	9:37	10:25	10:11	9:38	10:27	10:03	9:15
Ending local clock time (hh:mm)	12:05	12:31	11:50	11:31	12:19	12:07	11:24
Δt (min)	148.00	126.00	99.00	113.00	112.00	124.00	128.00
η_{avg}	0.09	0.11	0.25	0.09	0.11	0.08	0.08
F_2	0.19	0.21	0.47	0.18	0.20	0.16	0.13
$\dot{Q}^*_{50}$ (W)	30.9	31.9	33.7	30.7	31.7	30.4	22.3
$F'\ U_L/C$ (W/m^2 °C)	2.18	2.41	2.07	1.66	2.67	2.13	1.98
$F'\eta$ (W/m^2 °C)	0.21	0.24	0.22	0.18	0.24	0.21	0.18
COR (°C m^2/W)	0.098	0.098	0.105	0.111	0.090	0.100	0.089

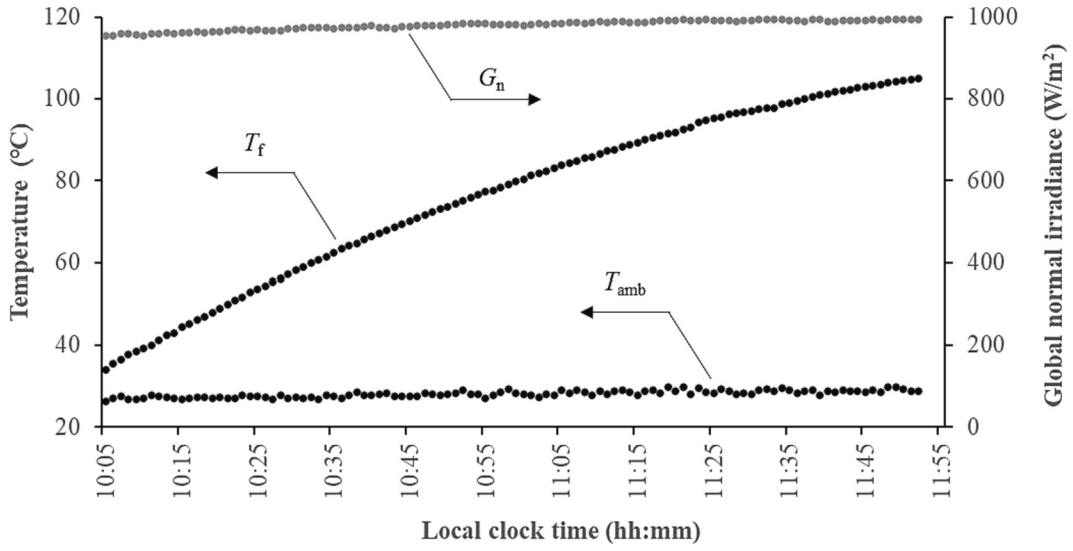

Fig. 11. Test performed with glycerin load with a glass enclosure on 19/7/2022.

detected are displayed in Fig. 7. The plot shows the correspondence between G_n and T_{amb} with the time taken by the water temperature to reach 90 °C. Fig. 8 illustrates the water temperature behavior of all the tests listed in Table 4 as a function of time. Although the tests were conducted on different days, with different conditions, all showed a concave function pattern. The water load test results showed that on 13/7/2022 test2 and 8/8/2023, using a pot enclosed with a glass bowl and a plastic bag, respectively, the times required to reach 90 °C from 40 °C were 94 min and 110 min. On the test of 19/07/2023 pro2, the water boiling temperature was reached after the longest time of 166 min, with the corresponding average G_n of 889.70 W/m^2 and average T_{amb} of 32.17 °C.

In addition to characterizing the cooking time of the tests, the cooking power and the optical-thermal ratio (*COR*) were determined. Fig. 9 shows the linear regression curve associated to the *cooking power* $\left(\dot{Q}^*_i\right)$ *as a function of* $\Delta T^*_{f,a,i}$ for the experimental tests conducted on 13/6/2022 and 17/7/2023 pro1. According to the approach of predicting cooking power calculation followed by Ruivo et al. (2022), all plots on this power curve figure were calculated with time intervals of 5 min. The values of $\dot{Q}^*_{50}$ were determined and summarized in Table 4. The highest and lowest values of $\dot{Q}^*_{50}$ were obtained during the tests with glass enclosure conducted on 13/6/22 and 21/7/23 and were determined to be 34.7 W and 21.8 W, respectively.

In Fig. 10, the efficiency (η) for the tests carried on 13/06/2022 and 17/7/2023 pro1 is depicted as a function of χ, which represents the ratio of the difference in temperature between water and ambient air to global normal irradiance, using a 5-min time interval. The efficiency curve's regression line and its associated coefficients, i.e., the parameters $F'\eta$ (the intercept of the line) and $F'U_L/C$ (the opposite value of the line's slope), were derived from the plotted points. These parameters were used to calculate the values of optical-thermal ratio (*COR*) reported in Table 4. The average values of *COR* for the glass and plastic enclosure tests were equal to 0.087 and 0.079 °C m^2/W, respectively.

Tests with glycerin

Four tests with the pot equipped with a glass enclosure and three with a plastic enclosure were conducted with 1 kg of glycerin. The

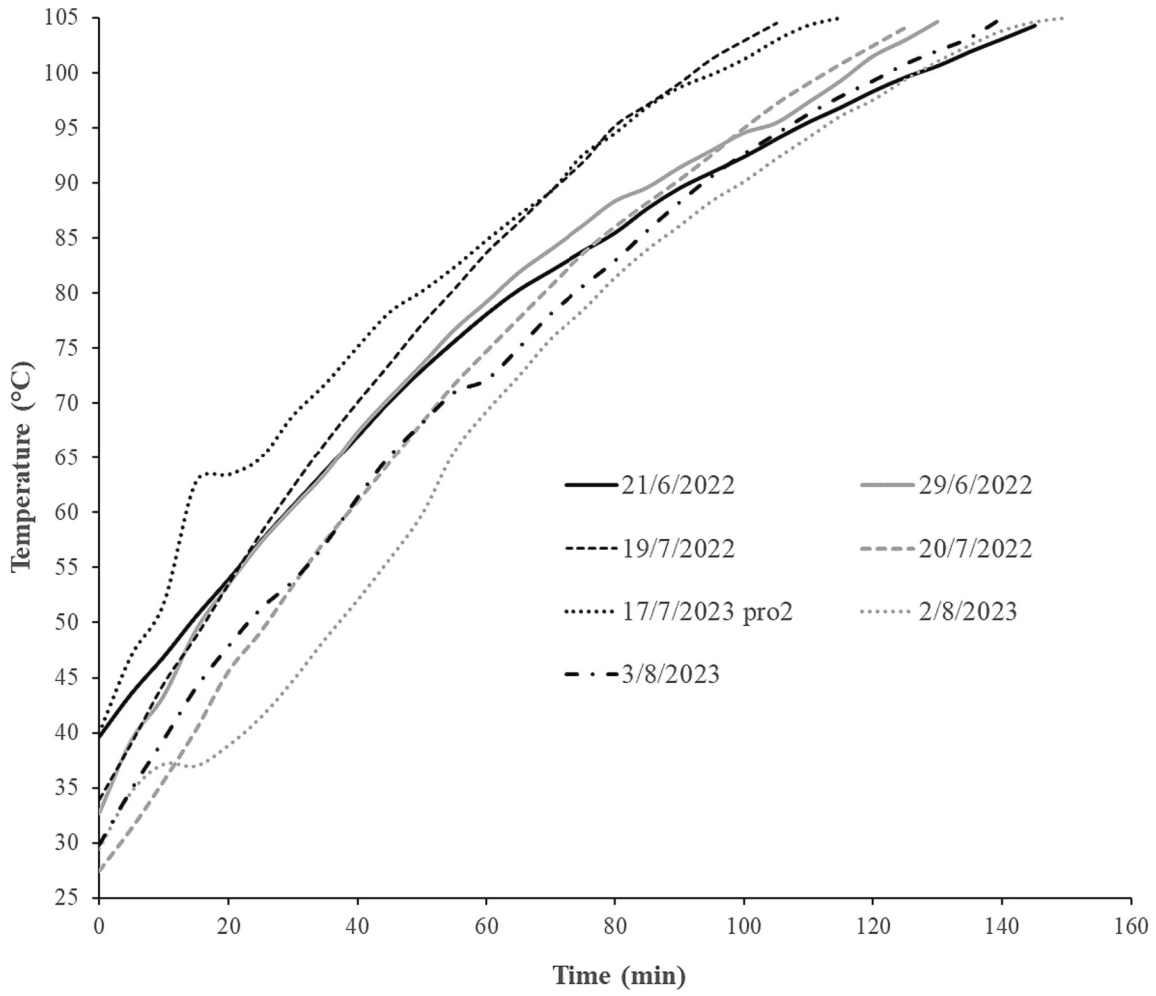

Fig. 12. Time evolutions of load temperature until 105 °C for all glycerin load tests. Details for the tests are reported in Table 5.

results obtained from the experiments are summarized in Table 5. The reported parameters and the arithmetic average values were calculated between 40 °C and 105 °C. The data indicates that the shortest time to attain the target temperature of 105 °C was achieved in the tests with a glass enclosure conducted on 19/7/2022. The results revealed that the test utilizing a pot with a glass enclosure took 99 min, with an average T_{amb} of 28.09 °C and an average G_n of 980.09 W/m^2. The second smallest time was recorded a pot enclosed with a plastic bag, required 112 min, conducted on 17/7/2023 pro2. The glycerin temperature and the global solar irradiance of the test on 21/06/2022 with the corresponding ambient temperature are shown in Fig. 11. The results of the glycerin load test similarly displayed a concave pattern of temperature for all experiments, despite the fluctuations in ambient temperature and global normal irradiance. This trend was consistent with the observations made during the water load test. Additionally, Fig. 12 provides a comprehensive illustration of the time needed to reach 105 °C for all tests (glass and a plastic bag enclosure).

The cooking power ($\dot{Q}_i^*$) and the optical-thermal ratio (*COR*) were calculated and reported in Table 5. Fig. 13 depicts the results of experimental tests conducted with a glass enclosure on 19/7/2022 and a plastic bag on 3/8/2023. It displays linear regression curve corresponding to the cooking power ($\dot{Q}_i^*$), with the associated values of $\Delta T_{f,a,i}^*$. The cooking power was calculated using the procedure used for the water tests, with 5 min time intervals. Additionally, Table 5 summarizes the cooking power ($\dot{Q}_{50}^*$) at 50 °C difference between the fluid temperature and T_{amb}, determined for each experimental test. The maximum and minimum values for $\dot{Q}_{50}^*$ were determined on 19/7/2022 and 3/8/2023 tests (33.7 W and 22.3 W, respectively).

Similar to water load test, Fig. 14 depicts the relationship between η and χ for the tests carried out on 19/7/2022 and 3/8/2023. Table 5 shows the $F'\eta_0$, $F'U_l/C$ and *COR* values for the glycerin load tests. It is possible to note that the *COR* values are comparable to those obtained during the water load test. The glass enclosure tests yielded an average *COR* of 0.103 °C m^2/W, while the plastic enclosure tests resulted in an average *COR* of 0.093 °C m^2/W.

Cooking tests

The effectiveness of the proposed cooker prototype was verified by using it to cook well-known and frequently used foods (i.e., tomatoes, rice, and potatoes). The black cooking pot enclosed with the glass bowl was used during the experiments. In the rice cooking test, an appropriate amount of water was added to the pot. Food temperature, ambient temperature, and solar irradiance were recorded during each test. The actual cooking time (Δt_c) was evaluated as the time needed by a food to reach its specific cooking temperature from ambient temperature. Table 6 presents the test conditions and the obtained cooking times. The behaviors of food temperature recorded in the cooking tests are shown in Fig. 15. It was found that the device could cook all the studied foods in less than two hours. In particular, the tomatoes took a shorter time (45 min) than rice (60 min) and potatoes (98 min). This outcome could be because the quantity of tomatoes cooked during the tests was smaller than those of rice and potatoes. The cooking time values of the proposed

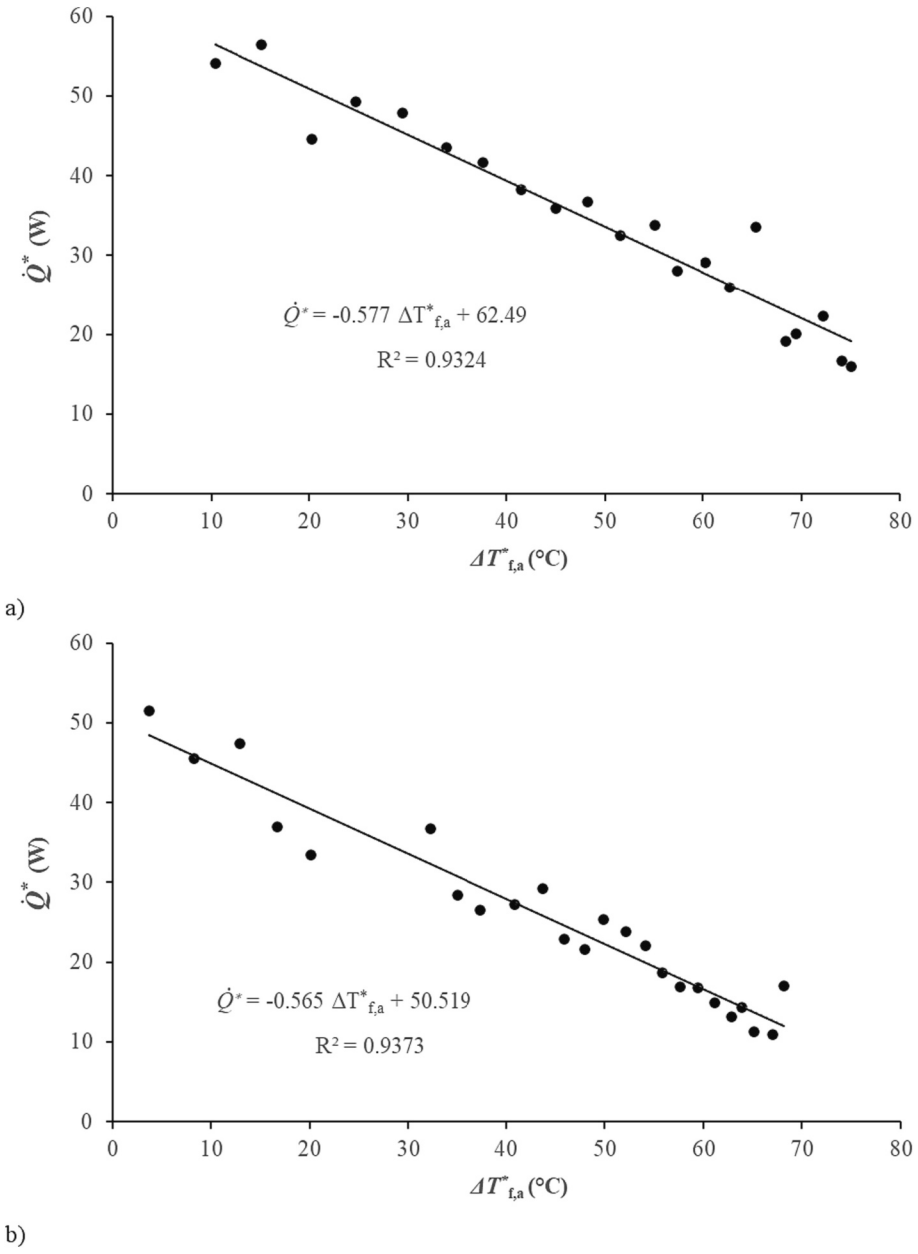

Fig. 13. Coking power curve as a function of temperature difference for the tests performed with glycerin: a) on 19/7/2022 with glass enclosure and b) on 3/8/2023 with plastic bag.

solar cooker agree well with the values provided by different solar box-type cookers described in the literature (Ademe & Hameer, 2018; Mahavar et al., 2012; Nahar, 2009). In particular, the box cooker investigated by Mahavar et al. (2012) was able to cook 400 g of rice in about 2 h, while the cooker developed by Ademe & Hameer (2018) cooked in 91 min 250 g of white rice and 500 g of potatoes in 95 min. Pictures of the cooked foods are reported in Appendix A.

Comparison with solar cookers presented in the literature

Table 7 compares the main features and performance parameters of the proposed cooking appliance with those of different foldable and small-sized solar cookers presented in the literature. The performance parameters for the proposed device reported in Table 7 are the average values of those given in Tables 3 and 4. It should be pointed out that it is not a trivial task to perform this kind of comparison, considering the different characteristics of the selected solar cookers. In addition, it was not possible to find all the analyzed performance parameters in the literature studies since various procedures were used to test the solar cookers.

Table 7 shows that the performance parameters of the presented cooker are slightly lower than those of the other prototypes. This outcome could be due to the lack of thermal insulation in the cooking chamber. Nevertheless, as proved by the results reported in previous sections, it ensures acceptable cooking performance. It is also evident that the proposed device is more compact than the other solar cookers when folded, proving that it is very easy to transport. Finally, the cost of the proposed device is lower or similar to that of the selected devices. It is also comparable to the prices of commercially available simple panel cookers, such as the Haines 2.0 Cooker with cooking pot, which costs about 100 US dollars (Haines Solar Cookers, 2024). It is worth pointing out that a direct comparison between the total cost of different solar cookers could not be very accurate because it is influenced by various factors, such as the different material and production costs in different countries.

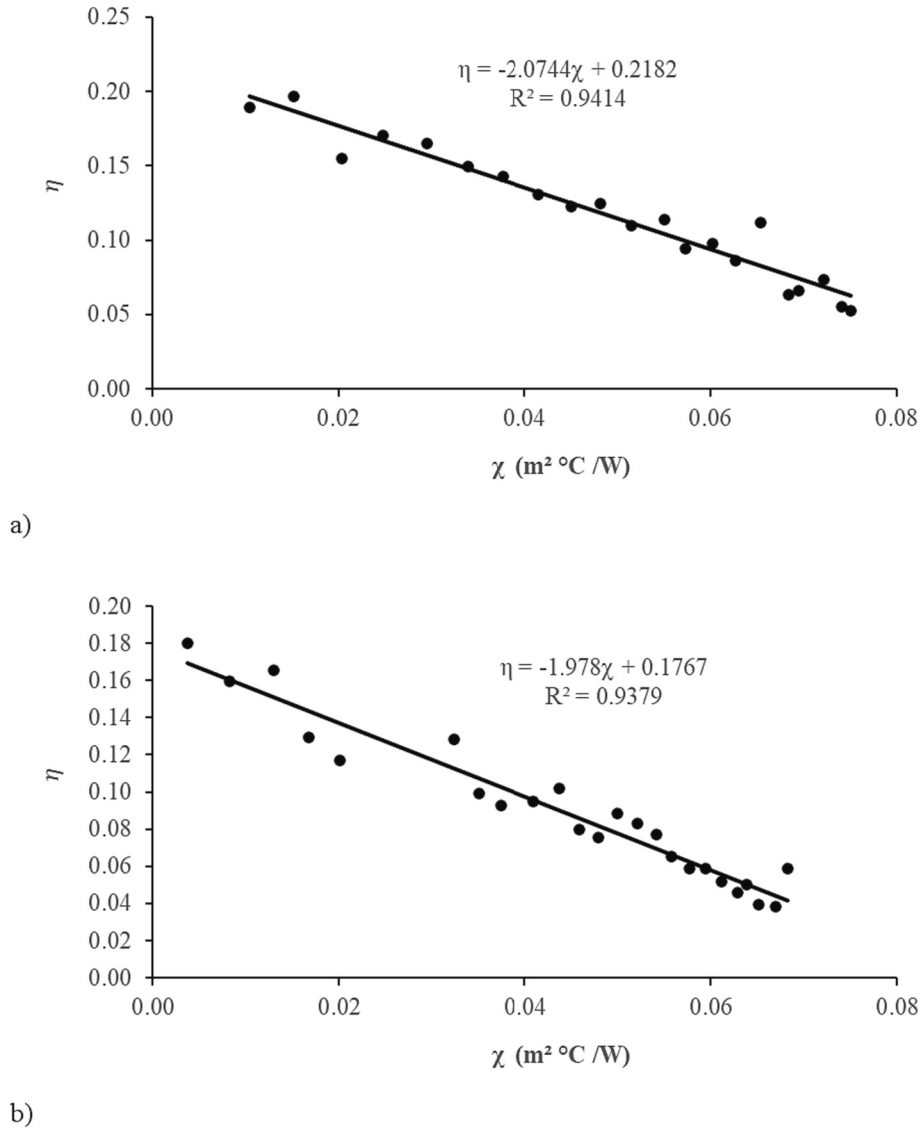

Fig. 14. Efficiency curve for the tests performed with glycerin: a) on 19/7/2022 with glass enclosure and b) on 3/8/2023 with plastic bag.

Table 6
Summary of the results of the cooking tests (the arithmetic average values were calculated between initial food temperature and cooking temperature).

Testing days	24/7/2023 pro1	19/7/2023 pro1	19/7/2023 pro2	20/7/2023 pro1
Food	Tomatoes	Rice	Potatoes	Potatoes
Mass (g)	104	200[a]	220	240
Cooking temperature (°C)	95	90	85	85
$G_{n,avg}$ (W/m^2)	984.71	847.32	922.07	954.86
$T_{amb,\ avg}$ (°C)	34.61	31.47	33.15	30.83
Starting local clock time (hh:mm)	11:37	10:19	11:35	10:26
Ending local clock time (hh:mm)	12:23	11:19	13:00	12:17
Δt_c (min)	46	60	85	111

[a] Rice was cooked with 150 g of water.

Conclusions

The prototype, which is characterized by its trapezoidal cooking chamber and adjustable reflector panels, has several advantages over existing solar cookers, as shown in Table 7. The design is simple, efficient, and easy to transport, making it ideal for use in remote and underserved communities, including humanitarian and refugee camps.

Despite having a low level of cooking power, the prototype demonstrates efficacy in the cooking of food and boiling of water. Additionally, the prototype has several strengths, including ease of mass production, compactness, and portability. Furthermore, the study emphasizes the potential for widespread use and adoption of solar energy for cooking purposes, particularly in developing countries and refugee camps. Moreover, with its low cost and ease of use, the solar cooker presents a sustainable and accessible solution for communities in need of a reliable source of cooking energy.

Finally, the authors recommend further study to explore the industrial processes, supply chain management, and socio-economic and cultural factors that could impact the implementation of this technology in vulnerable communities. The authors believe that a comprehensive understanding of these factors would lead to the effective implementation and widespread adoption of this technology, thereby contributing to sustainable energy solutions and improving the quality of life for communities in need.

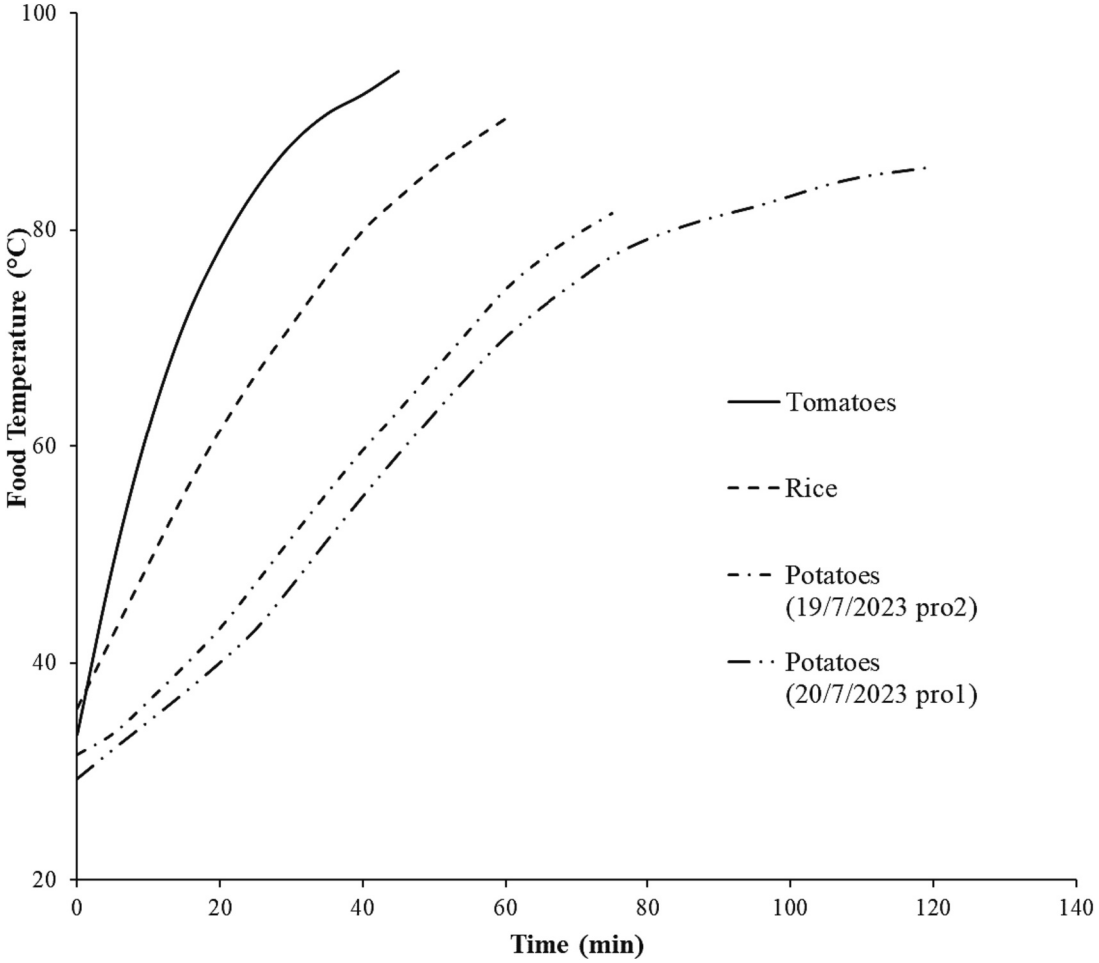

Fig. 15. Time evolutions of food temperature of the cooking tests.

Table 7
Comparison between the proposed solar cooker and various foldable and small-sized devices presented in previous studies.

	This study	Mahavar et al. (2012)	Folaranmi (2013)	Ademe & Hameer (2018)	Aquilanti et al. (2023)
Folded device dimensions (mm × mm × mm)	600 × 400 × 70	580 × 465 × 155	700 × 700 × 400	600 × 600 × 250	–
Device mass (kg)	7.0	8.0	–	–	–
A_a (m^2)	0.085	0.279	0.360	–	0.394–0.434
Cost (US dollars)	42	17[a]	–	196	208[b]
Test site	Ancona, Italy	Jaipur, India	Minna, Nigeria	Bahir Dar, Ethiopia	Ancona, Italy
Test period	May–July, 2022–2023	June–August 2009	March, 2013	March–April, 2017	May–June, 2021
Tests without load					
F_1 (°C m^2/W)	0.114[c]	0.116	0.110	0.123	0.110
Tests with water					
Pot type	Black stainless-steel pot enclosed with a glass bowl	Black aluminum pot	Black aluminum pot	Black stainless-steel pot	Black stainless-steel pot
Mass of water (kg)	1.0	1.2	2.0	1.4	2.0
η_{avg}	0.12	–	–	0.22	0.14
F_2	0.18	0.47	0.31	0.54	0.25
$\dot{Q}^*_{50}$ (W)	26.0	–	–	–	–
COR (°C m^2/W)	0.087	–	–	–	0.097

[a] Calculated from 1385 Indian rupees reported in the study considering an exchange rate of 0.012 US dollars/Indian rupees (January 2024).
[b] Calculated from 190 euros reported in the study considering an exchange rate of 1.09 US dollars/euros (January 2024).
[c] Tests carried out using a black pot within a glass enclosure.

Declaration of competing interest

The authors declare the following financial interests/personal relationships which may be considered as potential competing interests:

Claudia Paciarotti, Giovanni Di Nicola, Matteo Muccioli has patent #Removable, Resealable and Transportable Box-Type Solar Oven, 102,022,000,004,052 pending to Italy.

Appendix A. Examples of the cooked foods

Figs. A1, A2 and A3 show pictures of the cooked foods, i.e., tomatoes, rice, and potatoes.

a) b)

Fig. A1. Tomatoes: a) before cooking and b) after cooking.

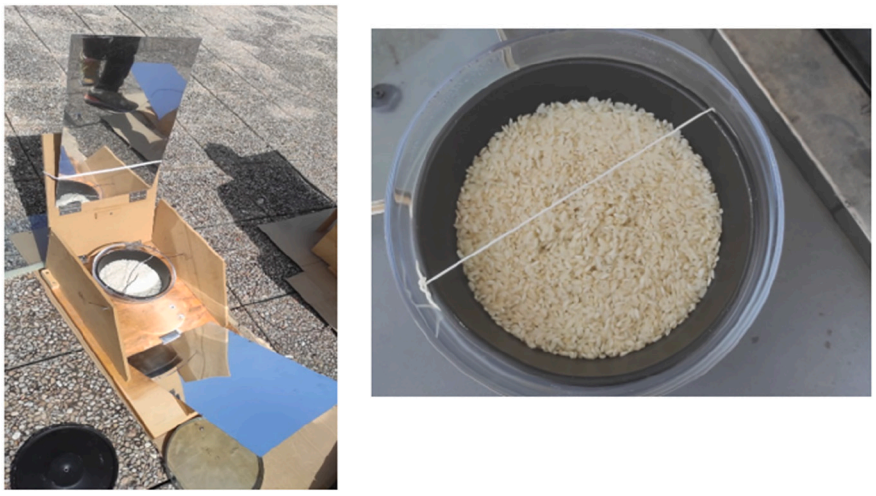

a) b)

Fig. A2. Rice: a) being cooked and b) after cooking (b).

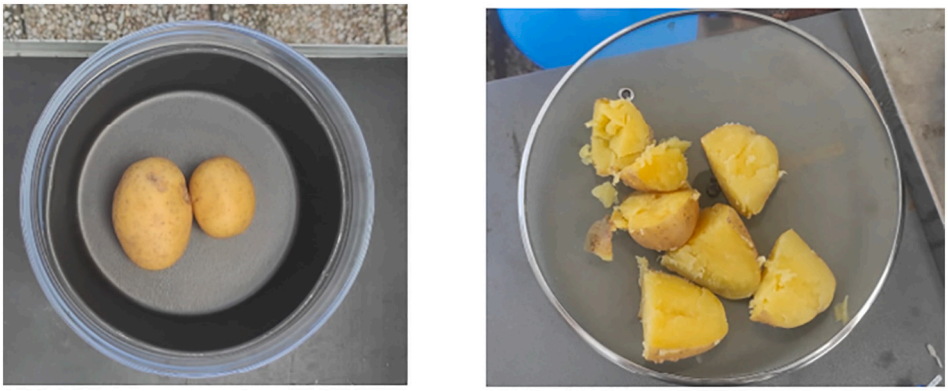

a) b)

Fig. A3. Potatoes: a) before cooking and b) after cooking.

References

Ademe, Z., & Hameer, S. (2018). Design, construction and performance evaluation of aBox type solar cooker with a glazing wiper mechanism. *AIMS Energy, 6*(1), 146–169. https://doi.org/10.3934/energy.2018.1.146

Aquilanti, A., Tomassetti, S., Muccioli, M., & Di Nicola, G. (2023). Design and experimental characterization of a solar cooker with a prismatic cooking chamber and adjustable panel reflectors. *Renewable Energy, 202*, 405–418. https://doi.org/10.1016/j.renene.2022.11.083

Arunachala, U. C., & Kundapur, A. (2020). Cost-effective solar cookers: A global review. *Solar Energy, 207*, 903–916. https://doi.org/10.1016/j.solener.2020.07.026

ASEAN Coordinating Centre for Humanitarian Assistance on Disaster Management, (2017). Catalogue and Brochure of DELSA Relief Items. Available at: https://ahacentre.org/wp-content/uploads/2017/03/AHACatalogue_Draft-09_highres_FA.compressed.pdf.

Battocchio, C., Bruni, F., Di Nicola, G., Gasperi, T., Iucci, G., Tofani, D., Varesano, A., & Venditti, I. (2021). Solar cookers and dryers: Environmental sustainability and nutraceutical content in food processing. *Foods, 10*(10), 2326. https://doi.org/10.3390/foods10102326

Berger, K., & Garyfalakis, E. (2013). *Procurement policies in disaster relief*. Jönköping: Jönköping International Business School.

Cerrahoğlu, M., & Maden, F. (2022). Design of transformable transitional shelter for post disaster relief. *International Journal of Disaster Resilience in the Built Environment.*. https://doi.org/10.1108/IJDRBE-05-2022-0049

Christopher, M. (2016). *Logistics and Supply Chain Management*. Pearson UK.

Costa, L. A., Rangel Carvalho, B., Lino Alves, J., Marques, A. T., da Silva, A. F. B., Esfandiari, P., & Parente, M. (2022). 4D structures for the short-time building of emergency shelters. *Proceedings of the Institution of Mechanical Engineers, Part L: Journal of Materials: Design and Applications, 236*(9), 1869–1894. https://doi.org/10.1177/14644207221086496

da Costa, S. R. A., Campos, V. B. G., & de Bandeira, R. A. M. (2012). Supply chains in humanitarian operations: Cases and analysis. *Procedia - Soc. Behav. Sci., 54*, 598–607. https://doi.org/10.1016/j.sbspro.2012.09.777

Duffie, J. A., & Beckman, W. A. (2013). *Solar engineering of thermal processes*. John Wiley & Sons.

Folaranmi, J. (2013). Performance evaluation of a double-glazed box-type solar oven with reflector. *J. Renew. Energy, 2013*, 1–8. https://doi.org/10.1155/2013/184352

Franceschi, J., Rothkop, J., & Miller, G. (2014). Off-grid solar PV power for humanitarian action: From emergency communications to refugee camp micro-grids. *Procedia Engineering, 78*, 229–235. https://doi.org/10.1016/j.proeng.2014.07.061

Funk, P. A. (2003). Testing and reporting solar cooker performance. *ASAE Stand.*, 825–826.

Funk, P. A., & Larson, D. L. (1998). Parametric model of solar cooker performance. *Solar Energy, 62*(1), 63–68. https://doi.org/10.1016/S0038-092X(97)00074-1

Haines Solar Cookers LLC. (2024) Haines 2.0 Solar Cooker with Cooking Pot. URL: https://hainessolarcookers.com/products/haines-2-solar-cooker (Accessed 15 January 2024).

International Federation of Red Cross and Red Crescent Societies (IFRC), (2017). Standard products catalogue. Available at: https://itemscatalogue.redcross.int/.

Joshi, S. B., & Jani, A. R. (2015). Design, development and testing of a small scale hybrid solar cooker. *Solar Energy, 122*, 148–155. https://doi.org/10.1016/j.solener.2015.08.025

Khalifa, A. M. A., Taha, M. M. A., & Akyurt, M. (1985). Solar cookers for outdoors and indoors. *Energy, 10*(7), 819–829. https://doi.org/10.1016/0360-5442(85)90115-X

Kovács, G., & Spens, K. M. (2007). Humanitarian logistics in disaster relief operations. *International Journal of Physical Distribution & Logistics Management, 37*(2), 99–114. https://doi.org/10.1108/09600030710734820

Lahn, G., & Grafham, O. (2015). Heat, light and power for refugees: Saving lives, reducing costs. *Chatham House Rep. Mov. Energy Initiat.*, 1–55.

Mahavar, S., Sengar, N., Rajawat, P., Verma, M., & Dashora, P. (2012). Design development and performance studies of a novel Single Family Solar Cooker. *Renewable Energy, 47*, 67–76. https://doi.org/10.1016/j.renene.2012.04.013

Mangan, J., Lalwani, C., & Butcher, T. (2008). *Global Logistics and Supply Chain Management*. John Wiley & Sons.

Martin, W. J., Hollingsworth, J. W., & Ramanathan, V. (2014). Household air pollution from cookstoves: Impacts on health and climate. *Glob. Clim. Chang. Public Heal.*, 237–255. https://doi.org/10.1007/978-1-4614-8417-2_13

Mercader-Moyano, P., & Porras-Pereira, P. (2023). Analysis of Contemporary Emergency Housing. In *Circular Economy in Emergency Housing: Eco-Efficient Prototype Design for Subaşi Refugee Camp in Turkey and Maicao Refugee Camp in Colombia: A Research Strategy of Climate Change* (pp. 47–66). Springer. https://doi.org/10.1007/978-3-031-32770-4_5.

Mirdha, U. S., & Dhariwal, S. R. (2008). Design optimization of solar cooker. *Renewable Energy, 33*(3), 530–544. https://doi.org/10.1016/j.renene.2007.04.009

Mullick, S. C., Kandpal, T. C., & Saxena, A. K. (1987). Thermal test procedure for box-type solar cookers. *Solar Energy, 39*(4), 353–360. https://doi.org/10.1016/S0038-092X(87)80021-X

Nahar, N. M. (2009). Design and development of a large size non-tracking solar cooker. *Journal of Engineering Science and Technology, 4*, 264–271.

Noyes, E. L., & Jones, O. B. (2019). *SolFly: Solar Energy Tent Fly for Humanitarian Aid*.

Paciarotti, C., Di Nicola, G., & Muccioli, M. (2022). Removable, Resealable and Transportable Box-Type Solar Oven, 102022000004052 [Online]. Available at: https://www.knowledge-share.eu/en/patent/removable-resealable-and-transportable-box-type-solar-oven/.

Padonou, E. A., Akabassi, G. C., Akakpo, B. A., & Sinsin, B. (2022). Importance of solar cookers in women's daily lives: A review. *Energy for Sustainable Development, 70*, 466–474. https://doi.org/10.1016/j.esd.2022.08.015

Panwar, N. L., Kaushik, S. C., & Kothari, S. (2011). Role of renewable energy sources in environmental protection: A review. *Renewable and Sustainable Energy Reviews, 15*(3), 1513–1524. https://doi.org/10.1016/j.rser.2010.11.037

Popescu, D.-A., Pereira, E., Givanovitch, G., Bakker, J., Pauwels, L., Dukoski, V., et al. (2021). In *Foldable Disaster Shelter-An EPS@ ISEP 2020 Project* (pp. 153–164).

Regattieri, A., Piana, F., Bortolini, M., Gamberi, M., & Ferrari, E. (2016). Innovative portable solar cooker using the packaging waste of humanitarian supplies. *Renewable and Sustainable Energy Reviews, 57*, 319–326. https://doi.org/10.1016/j.rser.2015.12.199

Rivoal, M., & Haselip, J. A. (2017). The true cost of using traditional fuels in a humanitarian setting. Case study of the Nyarugusu refugee camp, Kigoma region, Tanzania. *UNEP DTU Partnersh. Work. Pap. Ser., 3*, 1–42.

Rosenberg-Jansen, S. (2019). Leaving no one behind: An overview of governance of the humanitarian energy sector. *Energy Access and Forced Migration*, 15–33. https://doi.org/10.4324/9781351006941-3

Ruivo, C. R., Apaolaza-Pagoaga, X., Carrillo-Andrés, A., & Coccia, G. (2022). Influence of the aperture area on the performance of a solar funnel cooker operating at high sun elevations using glycerine as load. *Sustain. Energy Technol. Assessments, 53*, Article 102600. https://doi.org/10.1016/j.seta.2022.102600

Ruivo, C. R., Coccia, G., Di Nicola, G., Carrillo-Andrés, A., & Apaolaza-Pagoaga, X. (2022). Standardised power of solar cookers with a linear performance curve following the Hottel-Whillier-Bliss formulation. *Renewable Energy, 200*, 1202–1210. https://doi.org/10.1016/j.renene.2022.10.041

Safeer, M., Anbuudayasankar, S. P., Balkumar, K., & Ganesh, K. (2014). Analyzing transportation and distribution in emergency humanitarian logistics. *Procedia Eng., 97*, 2248–2258. https://doi.org/10.1016/j.proeng.2014.12.469

Sanglard, B., Lachaize, S., Carrey, J., & Tiruta-Barna, L. (2023). Life cycle assessment of a parabolic solar cooker and comparison with conventional cooking appliances. *Sustain. Prod. Consum., 42*, 211–233. https://doi.org/10.1016/j.spc.2023.09.018

Savonen, B., Mahan, T., Curtis, M., Schreier, J., Gershenson, J., & Pearce, J. (2018). Development of a resilient 3-D printer for humanitarian crisis response. *Technologies, 6*(1), 30. https://doi.org/10.3390/technologies6010030

Shao, J., Liang, C., Wang, X., Wang, X., & Liang, L. (2020). Relief demand calculation in humanitarian logistics using material classification. *International Journal of Environmental Research and Public Health, 17*(2), 582. https://doi.org/10.3390/ijerph17020582

Sitepu, T., Gunawan, S., Nasution, D. M., Ambarita, H., Siregar, R. E. T., & Ronowikarto, A. D. (2017). *Experimental study on performance of a box solar cooker with flat plate collector to boil water*. In . *180* p. 12032). https://doi.org/10.1088/1757-899X/180/1/012032

Smith, K. R., Bruce, N., Balakrishnan, K., Adair-Rohani, H., Balmes, J., Chafe, Z., … Rehfuess, E. (2014). Millions dead: How do we know and what does it mean? Methods used in the comparative risk assessment of household air pollution. *Annual Review of Public Health, 35*, 185–206. https://doi.org/10.1146/annurev-publhealth-032013-182356

Tatham, P., & Christopher, M. (2018). *Humanitarian logistics: Meeting the challenge of preparing for and responding to disasters*. Kogan Page Publishers.

Thomas, A. S., & Kopczak, L. R. (2005). From logistics to supply chain management: The path forward in the humanitarian sector. *Fritz Inst., 15*, 1–15.

Tiwari, G. N., & Yadav, Y. P. (1986). A new solar cooker design. *Energy Conversion and Management, 26*(1), 41–42. https://doi.org/10.1016/0196-8904(86)90029-4

U. E. 13698-1 Standard (2022). Euro pallets EPAL. [Online]. Available at: https://www.mecalux.com/warehouse-manual/pallet/euro-pallet.

UN Ocha. (2022). *Global Humanitarian Overview 2023*. Global Humanitarian Overview: United Nations. https://doi.org/10.18356/9789210024136

United Nations High Commissioner for Refugees (UNHCR) (2012). UNHCR Core Relief Items Catalogue. Available at: https://www.sheltercluster.org/sites/default/files/docs/UNHCR%20Core%20Relief%20Items%20Catalogue.pdf.